

Diploma Thesis

Non-Abelian Symmetries in the Numerical Renormalization Group

Arne Alex

October 12, 2009



Faculty of Physics
Ludwig-Maximilians-Universität München

I declare the thesis I am submitting is entirely my own work except where otherwise indicated, that I have clearly signalled the presence of quoted or paraphrased material and referenced all sources, and that it has not been submitted, either wholly or substantially, for another degree of this University, or for a degree at any other institution.

München, October 12, 2009

The present version of this thesis has undergone minor revisions and is not identical to the version given to the board of examiners.

First reviewer: Prof. Dr. Jan von Delft

Second reviewer: Prof. Dr. Gerhard Buchalla

Introduction

The *Numerical Renormalization Group*, or *NRG*, in short, has come a long way since its conception by Wilson in 1975. At that time, it was the first method to successfully solve the Kondo model, explaining the appearance of the Kondo effect in metals with magnetic impurities. After this preliminary success, another twenty years passed until the interest in NRG soared again when technology became advanced enough to fabricate devices on the nanoscale. In particular, quantum dots present a set-up which is tunable over a wide range of parameters, thus providing a new means to test quantum theories.

Transport through quantum dots can often be described by so-called impurity models, for which NRG remains the premier tool. Recent developments, e.g. obtaining a complete set of basis states [1], have drastically increased the precision of NRG, though computing time remains a limiting factor. It has been known for a long time [2] that certain Hamiltonians allow for a significant reduction of the run time by exploitation of symmetries. In this thesis, we tackle the problem of implementing NRG in a way that can take into account arbitrary unitary symmetries. Emphasis is put on $SU(N)$ symmetries, which would allow some multi-channel Kondo models to be treated efficiently for the first time.

The mathematical tool on which our approach is based is the *Wigner-Eckart theorem*, which simplifies the calculation of matrix elements of the Hamiltonian [3, 4]. This theorem, in turn, relies heavily on Clebsch-Gordan coefficients, which are familiar to physicists in the context of angular momentum coupling. In this context, the direct product of two irreducible representations (irreps) of the $SU(2)$ group is decomposed into a direct sum of irreps. $SU(3)$ Clebsch-Gordan coefficients arise, for example, in the context of QCD, and the Clebsch-Gordan coefficients for the group $SU(N)$, for general N , are useful for the numerical treatment of models with $SU(N)$ symmetry.

For explicit calculations with models having $SU(N)$ symmetry, explicit tables of $SU(N)$ Clebsch-Gordan coefficients are needed. Their calculation is a problem of the applied theory of representations of Lie groups that has been solved, in principle, long ago [5]. However, the relevant literature requires a rather detailed knowledge of the theory of Lie groups, going beyond that conveyed in the standard education of most physicists. And even with the requisite background, it is a nontrivial task to devise (and implement on a computer) an efficient algorithm for producing explicit

tables of $SU(N)$ Clebsch-Gordan coefficients for arbitrary N .

A major goal of this thesis is to present such an algorithm in a formulation accessible to physicists. We summarize the relevant facts from the representation theory of $SU(N)$ groups and explain how they can be combined into an efficient algorithm for calculating $SU(N)$ Clebsch-Gordan coefficients for arbitrary N . Since we need only ingredients that have already been proven in the mathematics literature, we refrain from reproducing any proofs. In fact, all of the needed ingredients can be found in textbooks on representation theory of Lie groups. Nevertheless, we are not aware of a text that assembles these ingredients in a concise way accessible to a physics readership, as we endeavor to do below.

We begin in Chapter 1 by giving a gentle introduction to symmetries of the Hamiltonian. Having put symmetries in a formal setting, we proceed to the idea of matrix representations, which naturally arise in the context of symmetries. After explaining how symmetries help to classify states and operators, we finish by stating the Wigner-Eckart theorem, our main tool for exploiting symmetries.

In Chapter 2, we concisely review the calculation of $SU(2)$ Clebsch-Gordan coefficients, well-known from the quantum mechanical theory of angular momentum. In doing so, we choose a strategy that can be readily generalized to the case of $SU(N)$.

The latter, of course, requires more general schemes for labeling the generators of the corresponding Lie algebra, its irreps and the states in each irrep. Such schemes are presented at the beginning of Chapter 3, followed by a statement of the desired algorithm.

Further on, we treat NRG in Chapter 4. Instead of following the original derivation, we introduce NRG with a strong focus on algorithmics and quickly traverse to the details of implementing symmetries in NRG.

We finish in Chapter 5 by summarizing our results and giving a brief overview of the projects to come.

Contents

Introduction	iii
1 Symmetries and representations	1
1.1 Symmetries	1
1.1.1 The symmetry group of the Hamiltonian	1
1.1.2 Unitary symmetries	3
1.1.3 Generators of symmetries	4
1.2 Representations	5
1.2.1 Definition	5
1.2.2 Representation vocabulary	5
1.2.3 Irreducible representations	6
1.2.4 Classification of states by symmetries	7
1.2.5 Labeling of states by eigenvalues of Casimir operators	8
1.2.6 Classification of operators by symmetries	9
1.2.7 Product representations	10
1.2.8 The Wigner-Eckart Theorem	11
2 Review of SU(2) Clebsch-Gordan coefficients	15
2.1 Angular momentum operators and matrix elements	15
2.2 General method for computing SU(2) Clebsch-Gordan coefficients	16
2.2.1 SU(2) product representations	16
2.2.2 Selection rule	17
2.2.3 Highest-weight states	18
2.2.4 Clebsch-Gordan series of SU(2)	19
2.2.5 Simple reducibility	20
2.2.6 Calculation of SU(2) Clebsch-Gordan coefficients	20
2.3 Alternative methods for obtaining SU(2) Clebsch-Gordan coefficients	21
2.3.1 Closed formula	22
2.3.2 Diagonalization of Casimir operators	22
3 Computation of SU(N) Clebsch-Gordan coefficients	23
3.1 The Lie algebra $\mathfrak{su}(N)$	23
3.2 Young tableaux techniques	24
3.2.1 Labeling of irreps by Young diagrams	24
3.2.2 Labeling of states by Young tableaux	25
3.2.3 Dimension of irreps	26
3.2.4 Irrep product decomposition	26
3.3 Gelfand-Tsetlin patterns	29

3.3.1	Correspondence to Young tableaux	29
3.3.2	Matrix elements of operators	33
3.4	Weights	34
3.4.1	Weight diagrams	34
3.4.2	Selection rule	36
3.4.3	Highest-weight states	36
3.4.4	Clebsch-Gordan coefficients with outer multiplicity	37
3.5	Generating lower-weight states of an irrep	38
3.6	Construction of all Clebsch-Gordan coefficients	39
3.6.1	Review of the algorithm	39
3.6.2	Consistency checks	40
4	Symmetries in the Numerical Renormalization Group	41
4.1	Structure of the Hamiltonian	41
4.2	Symmetries of the Hamiltonian	42
4.3	Statement of the algorithm	43
4.4	Reduced matrix elements of the initial Hamiltonian	45
4.5	Iterative construction of the Hamiltonian	47
4.5.1	Construction of states with good quantum numbers	47
4.5.2	Reduced matrix elements of the new Hamiltonian	48
4.5.3	Diagonalization and relabeling	49
4.6	Creation operator multiplets	49
5	Conclusions and Outlook	53
A	Mapping of irreps and states onto the natural numbers	55
A.1	Identifying Young diagrams with a single number	55
A.2	Mapping of Gelfand-Tsetlin patterns to matrix indices	58
B	Derivation of Eq. (4.15)	59
C	Program code for computing $SU(N)$ Clebsch-Gordan coefficients	61
C.1	Enumerating irreps	61
C.2	Mapping Gelfand-Tsetlin patterns to matrix indices	61
C.3	Dimension of an irrep	62
C.4	Matrix element of lowering operator	63
C.5	Construction of the lowering operator matrix	63
C.6	Weight vector	64
C.7	Clebsch-Gordan coefficients of the highest-weight state	65
C.8	Decomposition of a product representation	65
C.9	Calculation of the matrix of Clebsch-Gordan coefficients	66
	Bibliography	69
	Acknowledgements	77

Chapter 1

Symmetries and representations

Let A be an Hermitian operator that commutes with the Hamiltonian, $[H, A] = 0$. If $|a\rangle$ and $|a'\rangle$ are eigenstates with $A|a\rangle = a|a\rangle$ and $A|a'\rangle = a'|a'\rangle$, we immediately obtain

$$(a - a') \langle a' | H | a \rangle = 0. \quad (1.1)$$

In other words, the matrix elements of the Hamiltonian between states with different quantum numbers a and a' vanish. Within a suitable choice of basis, the Hamiltonian can be written as a block-diagonal matrix which has one block for each eigenvalue of A :

$$H = \begin{pmatrix} \boxed{H^{(a)}} & & & \\ & \boxed{H^{(a')}} & & \\ & & \ddots & \end{pmatrix}. \quad (1.2)$$

This simple fact allows us to save a lot of work because we can diagonalize each block individually instead of the whole Hamiltonian at once.

In the subsequent sections, we will review how this idea can be developed to a powerful method for exploiting symmetries based on the *Wigner-Eckart theorem*.

1.1 Symmetries

1.1.1 The symmetry group of the Hamiltonian

The set of all invertible operators (not necessarily Hermitian) which commute with the Hamiltonian forms a group, the so-called *symmetry group* of the Hamiltonian [6, p. 13]. The four group axioms are easily seen to hold true:

- The composition of operators is associative.

- The identity operator belongs to this set.
- Inverse elements exist by definition.
- If A and B are operators from this set, their composition also commutes with the Hamiltonian: $[H, AB] = 0$.

As an aside, we note $[H, A] = 0$ can also be written as $A^{-1}HA = H$ because any operator A belonging to this group is invertible. That is, the Hamiltonian is invariant under conjugation by A , from which it might be easier to see that it is also invariant with respect to AB .

Let us start with the most trivial example: The identity operator commutes with an arbitrary Hamiltonian and constitutes a group with one element. Every state is an eigenstate of the identity operator with eigenvalue 1, so, in analogy to Eq. (1.2), the Hamiltonian can be written as

$$H = \left(\begin{array}{c} \boxed{H^{(1)}} \end{array} \right). \quad (1.3)$$

Of course, this does not illustrate the advantages of exploiting symmetries. A better-known example is a particle in a central potential,

$$H = \frac{P^2}{2m} + V(|\mathbf{r}|), \quad (1.4)$$

which is invariant under spatial rotations. The symmetry group then includes the rotation operators, which are of the form $\exp(-i\mathbf{L} \cdot \boldsymbol{\omega})$, where $\mathbf{L} = (L_x, L_y, L_z)$ are the orbital angular momentum operators, and $\boldsymbol{\omega}$ is a vector specifying the angle and the axis of rotation. The blocks in the Hamiltonian can be labeled by two numbers l and m , where $l = 0, 1, \dots$ and $m = -l, \dots, l$, and the matrix elements $H_{nn'}^{(l,m)}$ in

each block, $H^{(l,m)}$, are distinguished by an additional quantum number, n :

$$H = \begin{pmatrix} \boxed{H^{(0,0)}} & & & & \\ & \boxed{H^{(1,1)}} & & & \\ & & \boxed{H^{(1,0)}} & & \\ & & & \boxed{H^{(1,-1)}} & \\ & & & & \ddots \end{pmatrix}. \quad (1.5)$$

Note that the rotation operators do not constitute the full symmetry group, which actually is the Lorentz group [7, p. 479]. However, any identification of a subgroup of the symmetry group takes us a step forward. We call a subgroup of the symmetry group a *symmetry*, in short.

1.1.2 Unitary symmetries

The symmetry of the central potential (Eq. (1.4)) is our first example of a *unitary symmetry*, which is a symmetry the elements of which are unitary. This is the case for the central potential because the Hermitian transpose of an operator of the form $\exp(-i\mathbf{L} \cdot \boldsymbol{\omega})$ is its inverse, $\exp(i\mathbf{L} \cdot \boldsymbol{\omega})$.

More precisely, the group of spatial rotations is isomorphic to the group $\text{SO}(3)$, the group of orthogonal 3×3 matrices with unit determinant [6, p. 6]. However, if we were not dealing with orbital angular momentum, but general angular momentum operators $\mathbf{J} = (J_x, J_y, J_z)$ which also admit half-integer eigenvalues, the symmetry group would be isomorphic to $\text{SU}(2)$ [7, p. 441]. As the special unitary groups $\text{SU}(N)$ play a central role in this thesis, we give their explicit definition here:

$$\text{SU}(N) = \left\{ U \in \mathbb{C}^{N \times N} \mid U^\dagger U = \mathbf{1}, \det U = 1 \right\}. \quad (1.6)$$

That is, $\text{SU}(N)$ is the group of unitary $N \times N$ matrices with unit determinant.

We would like to stress that, when we speak of $\text{SU}(N)$ being a symmetry of the Hamiltonian, we actually mean that one of the subgroups of the symmetry group of the Hamiltonian is isomorphic to $\text{SU}(N)$. However, which operators acting on the quantum states form this group has yet to be specified.

1.1.3 Generators of symmetries

To every Lie group, there exists an associated Lie algebra [7, p. 386]. For $SU(N)$, this is the Lie algebra $\mathfrak{su}(N)$, denoted by lower-case letters, which comprises the traceless anti-Hermitian $N \times N$ matrices:

$$\mathfrak{su}(N) = \left\{ A \in \mathbb{C}^{N \times N} \mid A^\dagger = -A, \operatorname{tr} A = 0 \right\}. \quad (1.7)$$

Frequently, we are rather going to use the *generators* of $SU(N)$, which are traceless Hermitian $N \times N$ matrices. If σ is a generator of $SU(N)$, then $i\sigma$ is an element of $\mathfrak{su}(N)$, and vice versa.

When trying to find a unitary symmetry of the Hamiltonian, it is usually easier to look for a set of operators corresponding to generators of a unitary group instead of the group itself. For this set, it is sufficient to fulfill the same commutation relations as their corresponding generators. The connection to the group is made via the exponential function, i.e. if σ is a generator of $SU(N)$, we have

$$i\sigma \in \mathfrak{su}(N) \iff \exp(i\sigma) \in SU(N). \quad (1.8)$$

However, this equivalence only holds for $SU(N)$, not arbitrary Lie groups [7, p. 390].

Let us finish this section with a well-known example. The Pauli matrices,

$$\sigma_x = \begin{pmatrix} 0 & 1 \\ 1 & 0 \end{pmatrix}, \quad \sigma_y = \begin{pmatrix} 0 & -i \\ i & 0 \end{pmatrix}, \quad \sigma_z = \begin{pmatrix} 1 & 0 \\ 0 & -1 \end{pmatrix}, \quad (1.9)$$

form a basis for the generators of $SU(2)$. Note that the generators constitute a *real* vector space, as complex linear combinations of the Pauli matrices are not necessarily anti-Hermitian. They have the following commutation relations:

$$[\sigma_k, \sigma_l] = 2i \sum_{m \in \{x,y,z\}} \epsilon_{klm} \sigma_m. \quad (1.10)$$

On the other hand, the operators J_x , J_y , and J_z obey, up to a constant, the same commutation relations:

$$[J_k, J_l] = i \sum_{m \in \{x,y,z\}} \epsilon_{klm} J_m. \quad (1.11)$$

So, if the latter operators commute with the Hamiltonian, we immediately obtain an $SU(2)$ rotational symmetry.

1.2 Representations

1.2.1 Definition

The idea behind a group representation is to find a matrix for every element of a group, so we can use ordinary matrix multiplication instead of the possibly complicated group multiplication rules while retaining the structure of the group. These matrices then form a group themselves, which canonically acts on \mathbb{C}^n (or \mathbb{R}^n) column vectors via matrix multiplication [6, p. 69]. However, we prefer to take the other way round in defining group representations.

We define a group representation Γ to be a homomorphism from a group \mathcal{G} to the automorphism group $\text{Aut}(\mathcal{H})$ of a vector space \mathcal{H} ,

$$\Gamma : \mathcal{G} \rightarrow \text{Aut}(\mathcal{H}). \quad (1.12)$$

The automorphism group $\text{Aut}(\mathcal{H})$ consists of all invertible linear operators acting on \mathcal{H} and is at the same time an algebra. To qualify as a group homomorphism, Γ must have the property that, if g and g' are elements of \mathcal{G} , then

$$\Gamma(g'g) = \Gamma(g')\Gamma(g). \quad (1.13)$$

This equation ensures that it does not matter whether we multiply two group elements before or after applying Γ and thus preserves the structure of the group.

The matrices representing the elements of \mathcal{G} are obtained as soon as we choose an orthonormal basis $\{|n\rangle\}$ of \mathcal{H} . For a given group element g , the matrix element between two basis states $|n\rangle$ and $|n'\rangle$ is given by $\langle n'|\Gamma(g)|n\rangle$. We will frequently refer to Γ as a matrix when the choice of basis does not matter, even though it is a mapping function in the proper sense.

Note that, in analogy to using generators instead of the symmetry group itself, we can also define a representation of a Lie algebra as a homomorphism from an algebra \mathcal{A} to the automorphism algebra of a vector space \mathcal{H} :

$$\Gamma : \mathcal{A} \rightarrow \text{Aut}(\mathcal{H}). \quad (1.14)$$

Here, an algebra homomorphism has to fulfill the following rules for a scalar $\lambda \in \mathbb{C}$ and any two elements $a, b \in \mathcal{A}$ [7, p. 405]:

$$\begin{aligned} \Gamma(\lambda a + b) &= \lambda\Gamma(a) + \Gamma(b), \\ \Gamma([a, b]) &= [\Gamma(a), \Gamma(b)]. \end{aligned} \quad (1.15)$$

1.2.2 Representation vocabulary

Let us briefly review various concepts arising in the representation theory of groups:

- The *carrier space* is the vector space denoted by \mathcal{H} above. In the context of quantum mechanics, we take a quantum state space as \mathcal{H} , but, in principle, this could be any vector space.
- The *dimension of a representation* is the dimension of the carrier space, which is also the size of the matrices which represent group elements. A *finite-dimensional representation* simply has a finite-dimensional carrier space. In this thesis, we will only consider finite-dimensional representations.
- A representation is called *unitary* if the matrices representing group elements are unitary. This applies to all representations we are interested in, as well.
- An injective representation is called *faithful*. We will deal with faithful as well as non-faithful representations, usually without specifying the difference.
- Two representations are *equivalent* if there exists a choice of basis in each carrier space such that the matrices representing group elements are the same. We do not distinguish between equivalent representations, i.e. when we speak of a representation, we implicitly refer to all equivalent representations as well. For example, all faithful representations on the same carrier space are equivalent.

1.2.3 Irreducible representations

It is desirable to classify all representations of a group. In principle, this is accomplished by finding all *irreducible representations* of the group, or *irreps*, in short, which are building blocks for all other representations.

Before we come to the definition of an irrep, we first need to introduce the idea of an *invariant subspace*: This is a subspace $\mathcal{H}' \subset \mathcal{H}$ of the carrier space \mathcal{H} of a representation Γ that is mapped onto itself by all group elements, i.e. $\Gamma(g)|n\rangle \in \mathcal{H}'$ for all $g \in \mathcal{G}$ and $|n\rangle \in \mathcal{H}'$. Clearly, \mathcal{H} itself and the subspace consisting of the null vector are examples, but we are rather interested in non-trivial subspaces.

If we can slice \mathcal{H} into two or more invariant subspaces (disjoint up to the null vector), the representation Γ is called *reducible*. Equivalently, all matrices $\Gamma(g)$ representing group elements can be made block-diagonal by a suitable choice of basis, where each invariant subspace results in another block, denoted, say, by Γ^k ,

in the matrix:

$$\Gamma(g) = \begin{pmatrix} \boxed{\Gamma^1(g)} & & & \\ & \boxed{\Gamma^2(g)} & & \\ & & \ddots & \\ & & & \ddots \end{pmatrix}. \quad (1.16)$$

Then, each invariant subspace constitutes the carrier space of another representation, say Γ^k , the matrices $\Gamma^k(g)$ of which are given by the block corresponding to this subspace. Such a block-diagonal representation is also called the *sum representation* of the representations given by the blocks.

In contrast, if the carrier space does not possess any invariant subspaces, or equivalently, if no choice of basis makes the matrices $\Gamma(g)$ block-diagonal all at once, we call the representation Γ *irreducible*. Whenever we encounter a reducible representation, our goal is to decompose it into its irreducible constituents.

1.2.4 Classification of states by symmetries

As the symmetry group of the Hamiltonian is a subgroup of the automorphism group $\text{Aut}(\mathcal{H})$ of the Hilbert space, we easily obtain representations of the symmetry group: The trivial embedding of the symmetry group into $\text{Aut}(\mathcal{H})$ serves well as the function Γ . This is why symmetries in quantum systems are intrinsically entwined with representation theory. The key idea is not to use the Hamiltonian to obtain representations of its symmetry group, but instead to do the opposite, namely, using representation theory to gain insight into the properties of the Hamiltonian and its eigenstates.

In most cases, this representation of the symmetry group is reducible, as sketched in Eq. (1.16), otherwise we would end up in the same situation as in Eq. (1.3). In the case of a reducible representation, each state that is a member of an invariant subspace of the symmetry group can be labeled by a *representation label*, denoting which block of the matrix representations they belong to, and an *internal label*, specifying how a state transforms under the action of the symmetry group. However, these two labels do not uniquely specify a state: There still might remain some degeneracy, in which case *additional labels* still are needed.

Let us illustrate this idea by an example: For the hydrogen atom, states are labeled by $|nlm\rangle$, where l is a representation label, m is an internal label, and n is an additional label. The representation and internal labels specify how angular momentum operators, e.g. L_x , act on a state,

$$L_x |nlm\rangle = \sum_{m'} \langle lm'|L_x|lm\rangle |nlm'\rangle, \quad (1.17)$$

where $\langle lm'|L_x|lm\rangle$ is a matrix element of the representation of the angular momentum operators specified by l . In principle, it would be more appropriate to write the matrix element $\langle lm'|L_x|lm\rangle$ as $\langle m'|\Gamma^l(L_x)|m\rangle$ because it is a matrix element of a matrix representation, but the former notation is common in the physics literature.

We would like to say few words about *multiplets*: Often, a set of states with equal energy, distinguished by different representation and internal labels, is referred to as a multiplet. We are rather going to refer to a multiplet as a set of states with the same representation label, distinguished by their internal label. In particular, if the states of such a multiplet are eigenstates of the Hamiltonian but the Hamiltonian breaks the corresponding symmetry, they will not be degenerate. Where this might lead to confusion, we will explicitly speak of *energy multiplets* or *symmetry multiplets*, respectively. For example, in atomic physics, degenerate s - and p -orbitals of a given shell are often referred to as a multiplet; we shall call this an energy multiplet. In contrast, for given n and l , the set of states $\{|nlm\rangle, m = -l, \dots, l\}$, will be called a symmetry multiplet, whose degeneracy is lifted, e.g. by an applied magnetic field that breaks rotational symmetry.

1.2.5 Labeling of states by eigenvalues of Casimir operators

Naturally, we would like to know which kind of representation and internal labels are necessary to describe the transformation properties of a state when we have identified a symmetry of the Hamiltonian. As sketched at the beginning of this chapter, these labels can be taken to be eigenvalues of operators belonging to the symmetry group. However, although each symmetry operator commutes with the Hamiltonian, they do not necessarily commute with each other. So, a state cannot simultaneously be an eigenstate of all symmetry operators.

Therefore, we seek a maximal set of commuting operators, e.g., for $SU(2)$, these are commonly taken to be J_z and \mathbf{J}^2 . Another example is given by the operator A of Eq. (1.1). In general, this set of operators consists of the *Casimir operators* [7, p. 592]. Let us assume that we can find M Casimir operators, denoted by $C_i, i = 1, \dots, M$, which all commute with the Hamiltonian and with each other. Then, a basis of the state space is given by the normalized simultaneous eigenstates of the Casimir operators, i.e. we label the basis states by $|n, c_1, \dots, c_M\rangle$ such that

$$C_i |n, c_1, \dots, c_M\rangle = c_i |n, c_1, \dots, c_M\rangle, \quad (1.18)$$

where n is an additional label distinguishing states having the same set of Casimir eigenvalues from each other. In the case of multiple, say M , Casimir operators, Eq. (1.1) should then be rewritten as

$$\langle n', c'_1, \dots, c'_M | H | n, c_1, \dots, c_M \rangle = \delta_{c'_1 c_1} \cdots \delta_{c'_M c_M} H_{n'n}^{(c_1, \dots, c_M)} \quad (1.19)$$

$j = 0$	$(\mathbb{1})$
$j = 1$	$(-J_+/\sqrt{2}, J_z, J_-/\sqrt{2})$
$j = 2$	$(J_+^2/2, -J_z J_+, (3J_z^2 - 1)/\sqrt{6}, J_z J_-, J_-^2/2)$

Table 1.1. Irreducible tensor operators arising in the decomposition of the space of operators acting on the states $|j = 1, m\rangle$. The components of an operator transforming as the irrep j is noted a tuple, $(T_j^j, T_{j-1}^j, \dots, T_{-j}^j)$.

Note that the set of Casimir eigenvalues includes internal as well as representation labels. As a consequence, only a subset of all Casimir operators are a multiple of the identity on an irreducible carrier space, and the eigenvalues of these Casimir operators can be used to specify the corresponding representation.

Finally, the eigenvalues of Casimir operators are not the only way to label states. For $SU(2)$, we use j as a representation label, instead of the proper eigenvalue $j(j+1)$. For $SU(N)$, we will even depart from taking numbers as symmetry labels, using graphical objects such as Young diagrams instead.

1.2.6 Classification of operators by symmetries

In the same way as representations of symmetries help us to classify quantum states, they also serve to classify operators acting on those states. For this purpose, we need a representation of the symmetry group the carrier space of which is the space $\text{End}(\mathcal{H})$, the space of linear operators (not necessarily invertible) acting on \mathcal{H} . By definition, the image $\Gamma(A)$ of an operator A in this representation acts on another operator B as follows [6, p. 112]:

$$\Gamma(A)B = A^{-1}BA. \quad (1.20)$$

That is, A is mapped onto an operator that acts on operators by conjugating them by A . This representation again allows us to slice the space of operators into invariant subspaces. A basis $\{T_m^j\}$ of such an invariant space is called an *irreducible tensor operator*, where j denotes a symmetry irrep. The dimension of this irrep is called the *rank* of the tensor operator.

For example, the state space which transforms as the $j = 1$ irrep of $SU(2)$ is three-dimensional, so the space of linear operators acting on this state space has $3^2 = 9$ dimensions. The representation given by Eq. (1.20) on this operator space is reducible and decomposes into a one-dimensional ($j = 0$), a three-dimensional ($j = 1$), and a five-dimensional ($j = 2$) representation [8, p. 242]. The respective irreducible tensor operators are shown in Table 1.1.

The most prominent example of an irreducible tensor operator is the Hamiltonian itself. As the Hamiltonian commutes with all symmetry operators, the matrix $\Gamma(A)$ in Eq. (1.21) must be the identity matrix. That is, Γ is the trivial irrep of the symmetry group, which maps each group element to the identity and is one-dimensional. An operator which transforms as this irrep is called a *scalar operator*.

Let us give a characterization of irreducible tensor operators which is much more convenient. Let $\{T_m^j\}$ be an irreducible tensor operator, where j denotes the irrep according to which the tensor operator T transforms and m indexes the components of the tensor operator. As an irreducible tensor operator constitutes an invariant subspace, conjugation of a given T_m^j by an operator of the symmetry group results in a linear combination of the full set $\{T_m^j\}$,

$$AT_m^j A^{-1} = \sum_{m'} \Gamma_{m'm}^j(A) T_{m'}^j, \quad (1.21)$$

where $\Gamma_{m'm}^j$ is called the matrix element of the irrep Γ^j between $T_{m'}^j$ and T_m^j [6, p. 112]. Instead of taking this equation as a definition for the matrix elements of Γ^j , we can as well take Eq. (1.21) as a definition of a tensor operator when the matrix elements $\Gamma_{m'm}^j$ have already been specified.

In general, the task of finding irreducible tensor operators is nontrivial. However, from already known tensor operators, we can construct new ones by reducing their product in terms in the same way as a product representation. We will address this issue briefly in Sec. 4.6.

1.2.7 Product representations

Before we finally approach the Wigner-Eckart theorem, we need to introduce the notion of *product representations* and of *Clebsch-Gordan coefficients*.

Given any two representations $\Gamma^p : \mathcal{G} \rightarrow \text{Aut}(\mathcal{H}_p)$ and $\Gamma^q : \mathcal{G} \rightarrow \text{Aut}(\mathcal{H}_q)$, we can form their *product representation* by taking the tensor product $\mathcal{H}_p \otimes \mathcal{H}_q$ of their carrier spaces. We denote this new representation by $\Gamma^{p \otimes q}$. The group elements then are mapped to the tensor product $\Gamma^p(g) \otimes \Gamma^q(g)$ of the respective operators. Furthermore, if $\{|n_p\rangle\}$ and $\{|n_q\rangle\}$ are bases of \mathcal{H}_p and \mathcal{H}_q , respectively, the representation matrices of the product representation in the basis given by all tensor products $\{|n_p \otimes n_q\rangle\}$ are obtained by taking the Kronecker product of the representation matrices of Γ^p and Γ^q , denoted by $\Gamma^p(g) \otimes \Gamma^q(g)$ as well.

There is an important difference between product representations of Lie groups and of Lie algebras: In the case of an algebra, we also take the tensor product of the carrier spaces for a product representation, but the algebra elements (or the generators) have to be mapped to $\Gamma^p(g) \otimes \mathbf{1} + \mathbf{1} \otimes \Gamma^q(g)$ for Eq. (1.8) still to be applicable.

Except in special cases, product representations are reducible, even if their composing factors are irreducible. One of the major goals of representation theory is to give rules for decomposing a product representation into a sum representation, i.e. finding the irreps occurring in the decomposition of a product representation, the so-called *Clebsch-Gordan series*. For $SU(2)$, this yields the well-known result,

$$j_1 \otimes j_2 = j_1 + j_2 \oplus j_1 + j_2 - 1 \oplus \cdots \oplus |j_1 - j_2|. \quad (1.22)$$

Note that, on the right-hand side, each irrep appears only once, a special property of $SU(2)$ that does not hold in general. The number of occurrences of a given irrep in such a decomposition is called its *outer multiplicity*.

The entries of a matrix C which performs the block-diagonalization of a product representation [6, p. 100],

$$C^{-1}(\Gamma^p(g) \otimes \Gamma^q(g))C = \bigoplus_k n_{pq}^k \Gamma^k, \quad (1.23)$$

where k runs over the Clebsch-Gordan series of this product representation and n_{pq}^k is the outer multiplicity of Γ^k , are called *Clebsch-Gordan coefficients*. The matrix C is usually chosen to be unitary and real [6, p. 104], which is possible through a suitable choice of the phases of the basis for the sum representation. The Clebsch-Gordan coefficients coincide for representations of the Lie group $SU(N)$ and of the Lie algebra $\mathfrak{su}(N)$ because, for each representation of $\mathfrak{su}(N)$, Eq. (1.8) leads to a representation of $SU(N)$ on the same carrier space, and Clebsch-Gordan coefficients are a property of the carrier space rather than of the matrices of a representation.

Clebsch-Gordan coefficients are well-known from angular momentum, where they normally are introduced as the overlap between states in a orthonormal basis $\{|j_1 m_1; j_2 m_2\rangle\}$ and states in another orthonormal basis $\{|j m\rangle\}$. A basis state from one basis can then be expanded in the another basis [8, p. 208],

$$|j m\rangle = \sum_{m_1, m_2} \langle j_1 m_1; j_2 m_2 | j m\rangle |j_1 m_1; j_2 m_2\rangle. \quad (1.24)$$

However, this notation is equivalent to the multiplication by the matrix C , written element-wise.

1.2.8 The Wigner-Eckart Theorem

The Wigner-Eckart theorem is the main tool for exploiting symmetries, relating individual matrix elements of irreducible tensor operators to each other.

Let $|n_1 j_1 m_1\rangle$ and $|n_2 j_2 m_2\rangle$ be states of the carrier spaces of irreps Γ^{j_1} and Γ^{j_2} of the symmetry group, respectively, i.e. j_1 and j_2 are representation labels, m_1 and

m_2 are internal labels, and n_1 and n_2 are additional labels. Furthermore, let T_m^j be an operator belonging to an irreducible tensor operator transforming as the irrep Γ^j , i.e. the matrices on the right-hand side of Eq. (1.21) belong to Γ^j . The matrix element of T_m^j between $|n_1 j_1 m_1\rangle$ and $|n_2 j_2 m_2\rangle$ then can be written as [6, p. 113]

$$\langle n_1 j_1 m_1 | T_m^j | n_2 j_2 m_2 \rangle = \sum_{\alpha=1}^{n_{j_1, j_2}^{j_1}} \langle j_2 m_2; j m | j_1 m_1 \alpha \rangle^* \langle n_1 j_1 || T^j || n_2 j_2 \rangle_{\alpha}, \quad (1.25)$$

where $\langle j_2 m_2; j m | j_1 m_1 \alpha \rangle$ is the Clebsch-Gordan coefficient of a state $|j_1 m_1\rangle$ appearing in the decomposition of the coupling of representations Γ^{j_2} and Γ^j , and α indexes the various occurrences of Γ^{j_1} in this decomposition, up to $n_{j_1, j_2}^{j_1}$, the outer multiplicity. (Note: The need to keep track of outer multiplicities does not apply to $SU(2)$, which is why this issue does not arise in standard quantum mechanics textbooks.) The quantity $\langle n_1 j_1 || T^j || n_2 j_2 \rangle_{\alpha}$ is a so-called *reduced matrix element*, which is a number no longer depending on the internal labels. It can be computed by [6, p. 311]

$$\langle n_1 j_1 || T^j || n_2 j_2 \rangle_{\alpha} = \frac{1}{d_{j_1}} \sum_{m_1} \sum_m \sum_{m_2} \langle j_2 m_2; j m | j_1 m_1 \alpha \rangle \langle n_1 j_1 m_1 | T_m^j | n_2 j_2 m_2 \rangle, \quad (1.26)$$

where d_{j_1} is the dimension of the carrier space of Γ^{j_1} , and the sums run over all states of the respective irrep. Formula (1.26) can be obtained by multiplying Eq. (1.25) by $\langle j_2 m_2; j m | j_1' m_1' \alpha' \rangle$ and summing over m_2 and m . The resulting formula still contains m_1 as a free variable. To avoid accidentally choosing m_1 such that the Clebsch-Gordan coefficient vanishes and the formula reduces to zero on both sides, we also sum over m_1 and divide by the number of terms in this sum, d_{j_1} . We finally exploit the following completeness relation for Clebsch-Gordan coefficients:

$$\sum_{m_2} \sum_m \langle j_1'' m_1'' \alpha'' | j_2 m_2; j m \rangle \langle j_2 m_2; j m | j_1' m_1' \alpha' \rangle = \delta_{j_1' j_1''} \delta_{m_1' m_1''} \delta_{\alpha' \alpha''}. \quad (1.27)$$

Let us turn to the interpretation of this theorem: Eq. (1.25) states that the matrix elements of an irreducible tensor operator between states of different irreps depend only on a restricted set of numbers, the reduced matrix elements. Their form is determined by dynamics (i.e. by the representation labels and additional labels, which are usually governed by the Hamiltonian of the problem). The precise form of the full matrix elements, beyond their dependence on the reduced matrix elements, is of a geometrical nature (i.e. determined purely by relevant representations of the symmetry group) and related to the reduced matrix elements via Clebsch-Gordan coefficients. In other words, this geometrical dependence can be factored out of the matrix elements. As soon as we know enough matrix elements of an irreducible

tensor operator to calculate the reduced matrix elements, the remaining matrix elements are determined by the Wigner-Eckart theorem.

Another considerable consequence concerns the diagonalization of the Hamiltonian. Eq. (1.1) follows directly from Eq. (1.25), because the Hamiltonian is a scalar operator of its symmetry group, implying that it cannot have matrix elements between two states with different symmetry labels. However, the Wigner-Eckart theorem goes a step further: Instead of keeping a matrix block for each pair of a representation label and an internal label, a single block referring to the representation label suffices. For example, returning to the SU(2) example of Eq. (1.5), we can represent the Hamiltonian in a block-diagonal form,

$$H = \begin{pmatrix} \boxed{H^{(0)}} & & & \\ & \boxed{H^{(1)}} & & \\ & & \boxed{H^{(2)}} & \\ & & & \ddots \end{pmatrix}, \quad (1.28)$$

in which each block $H^{(l)}$ contains as elements only the reduced matrix elements, $H_{nn'}^{(l)} = \langle nl || H || n'l \rangle$. Then we can diagonalize each block separately and reconstruct the full Hamiltonian afterwards, again by using the Wigner-Eckart theorem. This is much more efficient than using the form (1.5) because the latter contains many more blocks (since they carry labels l and m). (Alternatively, if one would use blocks labeled by l only, but without exploiting the Wigner-Eckart theorem, the blocks would be much larger, since the matrix elements $H_{nm,n'm'}^{(l)}$ would have to be labeled by a double index, n and m .)

By now, it should be clear that the use of symmetries can greatly speed up the process of diagonalizing a given Hamiltonian. Since this requires explicit knowledge of the Clebsch-Gordan coefficients, the major part of this thesis will be devoted to devising an algorithm for computing them explicitly for SU(N).

Chapter 2

Review of SU(2) Clebsch-Gordan coefficients

The material presented in this chapter is standard. A modern treatment can be found in [8], while the classic textbooks are those by [9] and [10].

2.1 Angular momentum operators and matrix elements

The angular momentum operators $\mathbf{J} = (J_x, J_y, J_z)$, which fulfill the commutation relations of Eq. (1.11), can be viewed as generators of SU(2). Moreover, we treat the operators $J_{\pm} = J_x \pm iJ_y$ and $\mathbf{J}^2 = J_x^2 + J_y^2 + J_z^2$ in the same manner, though they are not real linear combinations of the former, and thus formally are not generators of SU(2). The \mathbf{J}^2 operator is an example of a Casimir operator and, as such, commutes with all other angular momentum operators, $[\mathbf{J}^2, \mathbf{J}] = 0$. But the method for computing Clebsch-Gordan coefficients we are going to describe does not depend on \mathbf{J}^2 , so we are going to refer to it only occasionally.

On the other hand, the operators J_+ , J_z , and J_- are linearly independent and allow recovering J_x , J_y , and J_z by taking the appropriate complex linear combinations. Thus, we adopt as an equivalent definition of the generators of SU(2) the commutation relations

$$[J_z, J_{\pm}] = \pm J_{\pm}, \quad (2.1)$$

$$[J_+, J_-] = 2J_z. \quad (2.2)$$

We label the basis states on which they act by $|j, m\rangle$, where j is a non-negative half-integer, and m can assume the values $j, j-1, \dots, -j$. The $|j, m\rangle$ states are eigenstates of the J_z and \mathbf{J}^2 operators, and the matrix elements of these are given by ($\hbar = 1$)

$$\langle j' m' | \mathbf{J}^2 | j m \rangle = j(j+1) \delta_{j'j} \delta_{m'm}, \quad (2.3)$$

$$\langle j' m' | J_z | j m \rangle = m \delta_{j'j} \delta_{m'm}. \quad (2.4)$$

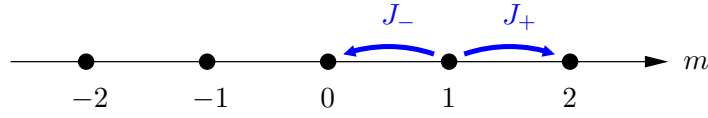


Figure 2.1. Depiction of the internal labels of the $j = 2$ irrep of $SU(2)$ on the x -axis. The J_- operator shifts a state to the left while the J_+ operator shifts to the right. The states with $m = -2$ and $m = 2$ are annihilated by J_- and J_+ , respectively.

The set of states $\{|j, m\rangle\}$ with fixed j forms the carrier space of a $2j + 1$ -dimensional $SU(2)$ representation, i.e. j is a representation label while m is an internal label. Remarkably, the representations labeled by j are irreducible and they are the only irreps of $SU(2)$, up to equivalence [6, p. 441].

The matrix elements of J_{\pm} are obtained by a few simple considerations [8, p. 191]. First, we note that $J_z J_{\pm} |jm\rangle = (m \pm 1) J_{\pm} |jm\rangle$, provided that $m \neq \pm j$. Then, we evaluate the norm of $J_{\pm} |jm\rangle$ by the use of $\langle jm | J_{\pm}^{\dagger} J_{\pm} |jm\rangle = \langle jm | (\mathbf{J}^2 - J_z^2 \mp J_z) |jm\rangle$. By choosing the matrix elements to be real and positive, we obtain

$$\langle j' m' | J_{\pm} |jm\rangle = \sqrt{(j \pm m + 1)(j \mp m)} \delta_{j'j} \delta_{m', m \pm 1}. \quad (2.5)$$

The operators J_{\pm} are called *ladder operators* or *raising and lowering operators* for their effect of raising or lowering the internal label m of a state $|jm\rangle$ by one unit, as shown in Fig. 2.1.

2.2 General method for computing $SU(2)$ Clebsch-Gordan coefficients

2.2.1 $SU(2)$ product representations

Let us plunge right into the problem of decomposing $SU(2)$ product representations. In a quantum physics context, this is rather known as the *coupling of angular momenta*, which is why we will sometimes speak of “coupling” irreducible representations.

Starting from two angular momentum representations, i.e. a set of states $|j_1 m_1\rangle$ and operators J_{1z} and $J_{1\pm}$ acting on them, plus a set of states $|j_2 m_2\rangle$ and the corresponding operators J_{2z} and $J_{2\pm}$, we form the tensor product of the spaces spanned by the two sets of states. This product space is, in turn, spanned by all tensor products of the form $|j_1 m_1\rangle \otimes |j_2 m_2\rangle$, which we will denote by $|j_1 m_1; j_2 m_2\rangle$, in short. Furthermore, we define total angular momentum operators $J_z = J_{1z} \otimes \mathbf{1} + \mathbf{1} \otimes J_{2z}$ and $J_{\pm} = J_{1\pm} \otimes \mathbf{1} + \mathbf{1} \otimes J_{2\pm}$.

The total angular momentum operators fulfill the same commutation relations as in Eq. (1.11) [8, p. 207]. They thus give rise to another representation of the $SU(2)$ generators on the carrier space spanned by the states $|j_1 m_1; j_2 m_2\rangle$, which is the product representation $j_1 \otimes j_2$ of the $SU(2)$ irreps labeled by j_1 and j_2 . Let Γ^{j_1} and Γ^{j_2} be the matrices of any of the operators J_z or J_{\pm} in the irreps j_1 and j_2 , respectively, then the matrix $\Gamma^{j_1 \otimes j_2}$ is given by

$$\Gamma^{j_1 \otimes j_2} = \Gamma^{j_1} \otimes \mathbb{1} + \mathbb{1} \otimes \Gamma^{j_2}, \quad (2.6)$$

where \otimes denotes the Kronecker product of two matrices. As noted in Sec. 1.2.7, the product representation $\Gamma^{j_1 \otimes j_2}$ is, in general, reducible, and we seek to decompose it into its irreducible constituents.

Therefore, our first goal is to find all irreps occurring in the decomposition of $\Gamma^{j_1 \otimes j_2}$, the so-called Clebsch-Gordan series. Although we have anticipated the result in Eq. (1.22), we are going to derive the Clebsch-Gordan series of $SU(2)$ in detail.

Our second goal is to compute the matrix C of Clebsch-Gordan coefficients, as in Eq. (1.23), which block-diagonalizes the product representation,

$$C^\dagger \Gamma^{j_1 \otimes j_2} C = \begin{pmatrix} \boxed{\Gamma^{j_1+j_2}} & & & & \\ & \boxed{\Gamma^{j_1+j_2-1}} & & & \\ & & \ddots & & \\ & & & & \boxed{\Gamma^{|j_1-j_2|}} \end{pmatrix}. \quad (2.7)$$

We will call each representation appearing on the right-hand side a *target irrep*.

Recall that we label states of an $SU(2)$ irrep carrier space by $|jm\rangle$, so the block-diagonalization can as well be written as a basis transformation of the carrier space,

$$|jm\rangle = \sum_{m_1, m_2} \langle j_1 m_1; j_2 m_2 | jm \rangle |j_1 m_1; j_2 m_2\rangle, \quad (2.8)$$

which is the expression we are going to work with, rather than Eq. (2.7).

2.2.2 Selection rule

As an important stepping stone, we observe that a Clebsch-Gordan coefficient $\langle j_1 m_1; j_2 m_2 | jm \rangle$ vanishes unless

$$m_1 + m_2 = m. \quad (2.9)$$

This follows from bracketing both sides of $J_z = J_{1z} + J_{2z}$ by $\langle j_1 m_1; j_2 m_2 |$ and $|jm\rangle$ [8, p. 208].

As a consequence, only relatively few Clebsch-Gordan coefficients are non-zero, and thus, the matrix C of Eq. (2.7) is sparsely populated. Moreover, we can drop one of the sums in Eq. (2.8) by eliminating m_1 or m_2 through this selection rule.

2.2.3 Highest-weight states

For each $SU(2)$ irrep j , the state $|jj\rangle$ is called the *highest-weight state*, since

$$J_+ |jj\rangle = 0. \quad (2.10)$$

When expanding the highest-weight state of a target irrep of a product representation decomposition in terms of the old basis states $|j_1 m_1; j_2 m_2\rangle$, this property remains valid, i.e.

$$J_+ \sum_{m'} c_{m'} |j_1, m_1; j_2, j - m'\rangle = 0, \quad (2.11)$$

where $c_{m'}$ are the expansion coefficients, and the sum runs over all values for which $\max\{-j_1, j - j_2\} \leq m_1 \leq \min\{j_1, j + j_2\}$. By letting $J_+ = J_{1+} + J_{2+}$ act on the states $|j_1, m'; j_2, j - m'\rangle$ in Eq. 2.11 and multiplying by $\langle j_1, m'' + 1; j_2, j - m'' |$ from the left, we obtain

$$\begin{aligned} & \sqrt{(j_1 - m'')(j_1 + m'' + 1)} c_{m''} \\ & + \sqrt{(j_2 - j + m'' + 1)(j_2 + j - m'')} c_{m''+1} = 0, \end{aligned} \quad (2.12)$$

which is a system of linear equations in the Clebsch-Gordan coefficients $c_{m''}$ of the state $|jj\rangle$. Actually, this system is bidiagonal and can be rewritten as a recursion relation,

$$c_{m''} = -\sqrt{\frac{(j_2 - j + m'' + 1)(j_2 + j - m'')}{(j_1 - m'')(j_1 + m'' + 1)}} c_{m''+1}, \quad (2.13)$$

and thus leaves only one degree of freedom, e.g. the coefficient c_j . To ultimately determine the Clebsch-Gordan coefficients, we take into account the normalization condition

$$\sum_{m'} |c_{m'}|^2 = 1, \quad (2.14)$$

which must hold for any state, and choose the Clebsch-Gordan coefficients to be real. Still, certain sign conventions have to be specified [8, p. 211], but anyone is fine as long as we stick to it consistently.

The system of linear equations given in Eq. (2.12) provides a possibility to calculate an initial set of Clebsch-Gordan coefficients as well as to figure out which irreps j occur in the decomposition of an $SU(2)$ product representation, namely those for which Eq. (2.12) has a solution.

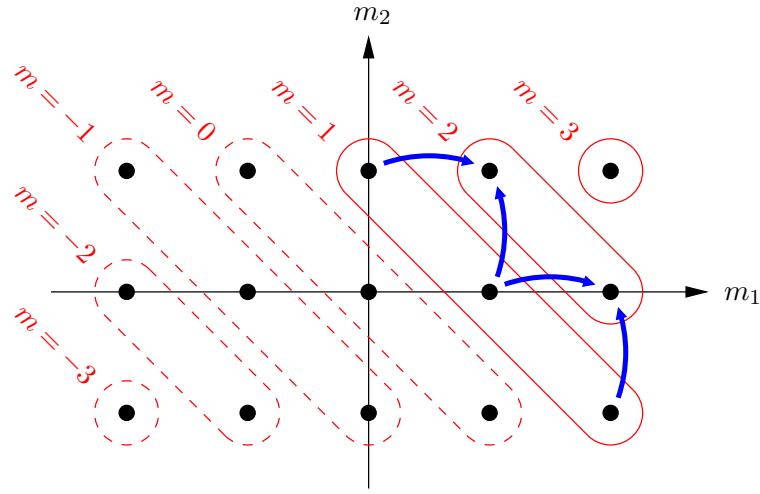


Figure 2.2. m_1 - m_2 -plane for the case $j_1 = 2$, $j_2 = 1$. Points with fixed total m are encircled, with solid or dashed lines if $m \geq |j_1 - j_2|$ or $m < |j_1 - j_2|$, respectively. Horizontal and vertical arrows indicate the action of J_{1+} and J_{2+} , respectively.

2.2.4 Clebsch-Gordan series of $SU(2)$

Evidently, the selection rule Eq. (2.9) prohibits states with $m > j_1 + j_2$, so only irreps with $j \leq j_1 + j_2$ can appear in a decomposition. We can convince ourselves that the irrep $j = j_1 + j_2$ does indeed occur because there exists only one state with $m = j_1 + j_2$, namely $|j_1 j_1; j_2 j_2\rangle$, so we have

$$|j_1 + j_2, j_1 + j_2\rangle = |j_1 j_1; j_2 j_2\rangle. \quad (2.15)$$

As soon as we find the highest-weight state of any irrep in terms of the old basis states, we are guaranteed that this irrep occurs in the decomposition [7, p. 612] because the highest-weight state must belong to an invariant subspace of the product representation carrier space, and we can always find the other basis states of this invariant subspace by applying the lowering operator J_- to the highest-weight state.

In general, we can visualize the construction of a highest-weight state as in Fig. 2.2. For a trial target irrep j , we seek a linear combination of the states $|j_1 m_1; j_2 m_2\rangle$ with $m_1 + m_2 = j$ which is annihilated by the J_+ operator, as in Eq. (2.11). In Fig. 2.2, this corresponds to taking a linear combination of the states located on the diagonal $m = j$. The operators J_{1+} and J_{2+} map each state $|j_1 m_1; j_2 m_2\rangle$ to its horizontal and vertical neighbor, respectively, so the linear combination of states with $m_1 + m_2 = j$ is mapped to a linear combination of the states with

$m_1 + m_2 = j + 1$. For example, the set of states with $m = 1$ is mapped to the set of states with $m = 2$, as indicated by the arrows in Fig. 2.2.

For the linear combination of the diagonal $m = j + 1$, which is obtained by applying the J_+ to the linear combination of the diagonal $m = j$, to vanish, the prefactor of each linearly independent state must be zero, which is expressed by Eq. (2.12). For a single state on the $m = j + 1$ diagonal, this can be accomplished if it can be reached in two different ways from the $m = j$ diagonal, which can be made to cancel by appropriate choice of the coefficients of the linear combination (leading to Eq. (2.13)). However, if any state on the $m = j + 1$ diagonal can be reached in only one way, it is no longer possible to compensate this contribution by modifying another prefactor.

In consequence, Eq. (2.12) has a non-trivial solution if and only if the diagonal $m = j$ is longer than the diagonal $m = j + 1$ in the picture corresponding to Fig. 2.2. This is the case for the diagonals encircled by solid lines in Fig. 2.2. It is not hard to geometrically figure out for which diagonals, and thereby for which values of j , we can find a highest-weight state, namely for

$$j = j_1 + j_2, j_1 + j_2 - 1, \dots, |j_1 - j_2|, \quad (2.16)$$

which is the same result as in Eq. (1.22).

2.2.5 Simple reducibility

In principle, it would be possible that the linear system given in Eq. (2.12) has more than one non-trivial solution, and thus, an $SU(2)$ irrep would occur more than once in a decomposition. Let us give two short arguments why this is not the case.

As mentioned in Sec. 2.2.3, the system of linear equations in Eq. (2.12) is bidiagonal and, as such, has a single degree of freedom. Thus, there cannot exist two independent solutions. Another illustrative reasoning is the check of dimensions [8, p. 209]: The dimensions of the irreps occurring in a decomposition must add up to the product of the dimensions of the two factors of the product representation, i.e.

$$\sum_{j=j_1-j_2}^{j_1+j_2} (2j+1) = (2j_1+1)(2j_2+1). \quad (2.17)$$

The fact that each irrep j appears only once, also called *simple reducibility* is a particular feature of $SU(2)$. For $SU(3)$ and above, this will no longer be valid.

2.2.6 Calculation of $SU(2)$ Clebsch-Gordan coefficients

After solving Eq. (2.12) for the Clebsch-Gordan coefficients of the state $|jj\rangle$, we are almost done. The Clebsch-Gordan coefficients of a state $|jm\rangle$ are obtained by

acting with J_- on both sides of the expansion of $|jj\rangle$ in the old basis states,

$$|jj\rangle = \sum_{m'} c_{m'} |j_1, m'; j_2, j - m'\rangle. \quad (2.18)$$

Care has to be taken to divide by the prefactors introduced by J_- , though they are the same on both sides. In particular, a state $|jm\rangle$ is reached from $|jj\rangle$ by

$$|jm\rangle = \sqrt{\frac{(j+m)!}{(j-m)!(2j)!}} (J_-)^{j-m} |jj\rangle. \quad (2.19)$$

Combining Eqs. (2.18) and (2.19), [8, p. 211] gives a simple recursion relation for the Clebsch-Gordan coefficients of a target irrep j , which can be used for explicit calculations, once the Clebsch-Gordan coefficients of the highest-weight state have been found:

$$\begin{aligned} & \sqrt{(j \mp m)(j \pm m + 1)} \langle j_1 m_1; j_2 m_2 | j, m \pm 1 \rangle \\ &= \sqrt{(j_1 \mp m_1 + 1)(j_1 \pm m_1)} \langle j_1, m_1 \mp 1; j_2 m_2 | jm \rangle \\ & \quad \sqrt{(j_2 \mp m_2 + 1)(j_2 \pm m_2)} \langle j_1 m_1; j_2, m_2 \mp 1 | jm \rangle \end{aligned} \quad (2.20)$$

$SU(N)$ Clebsch-Gordan coefficients can be obtained by following essentially the same strategy, of first determining the highest-weight states explicitly and then systematically applying lowering operators. However, more elaborate schemes for labeling the generators of the groups, its irreps and the states in each irrep need to be developed. It turns out that this can be done very conveniently using graphical tools such as Young diagrams, Young tableaux and Gelfand-Tsetlin patterns, which will be introduced in the next chapter.

2.3 Alternative methods for obtaining $SU(2)$ Clebsch-Gordan coefficients

Due to the fact that $SU(2)$ is simply reducible, several more elegant methods for calculating $SU(2)$ Clebsch-Gordan coefficients are known, of which we are going to present two. Note, though, that the method we have described in the previous section generalizes most easily to $SU(N)$.

j	m	$j(j+1)$	$j(j+1)+m$
0	0	0	0
1/2	-1/2	3/4	1/4
1/2	1/2	3/4	5/4
1	-1	2	1
1	0	2	2
1	1	2	3
\vdots	\vdots	\vdots	\vdots

Table 2.1. Eigenvalues of the first few states $|jm\rangle$ with respect to the operator $\mathbf{J}^2 + J_z$. Each state can be uniquely identified by its eigenvalue, which is displayed in the rightmost column.

2.3.1 Closed formula

Several authors have given closed formulas for $SU(2)$ Clebsch-Gordan coefficients [7, p. 458], e.g.

$$\begin{aligned}
\langle j_1 m_1; j_2 m_2 | j m \rangle &= ((2j+1)(j_1+j_2-j)!(j_1-j_2+j)!(j-j_1+j_2)!)^{\frac{1}{2}} \\
&\quad \times ((j_1+m_1)!(j_1-m_1)!(j_2+m_2)!(j_2-m_2)!(j+m)!(j-m)!)^{\frac{1}{2}} \\
&\quad \times \sum_{m'} (-1)^{m'} (m'!(j_1+j_2-j-m')!(j_1-m_1-m')!(j_2+m_2-m')! \\
&\quad \times (j-j_2+m_1+m')!(j-j_1+m_2+m')!(j_1+j_2+j+1)!)^{-\frac{1}{2}} \quad (2.21)
\end{aligned}$$

While this formula is convenient for computing isolated Clebsch-Gordan coefficients, it will be computationally more expensive than other approaches when the full set of Clebsch-Gordan coefficients of a product representation decomposition is needed.

2.3.2 Diagonalization of Casimir operators

For a short implementation in computer algebra systems, it is convenient to diagonalize [11]

$$\mathbf{J}^2 + J_z = (\mathbf{J}_1^2 + J_{1z}) \otimes \mathbf{1} + \mathbf{1} \otimes (\mathbf{J}_2^2 + J_{2z}). \quad (2.22)$$

Each state $|jm\rangle$ has a unique eigenvalue with respect to this operator, as shown in Table 2.1. This allows states with equal m in a product representation decomposition to be distinguished from each other, and each such state to be unambiguously assigned to the irrep labeled by the corresponding j . The matrix which diagonalizes this operator in the product representation is exactly the desired matrix of Clebsch-Gordan coefficients.

Chapter 3

Computation of $SU(N)$ Clebsch-Gordan coefficients

Constructing an algorithm to calculate arbitrary $SU(N)$ Clebsch-Gordan coefficients proved harder than anticipated. While a lot of introductory literature on representation theory is available, from a mathematical point of view [12, 13, 14] as well as written by physicists [15, 16, 6, 7], few books explicitly treat the calculation of $SU(N)$ Clebsch-Gordan coefficients, and even fewer do so from an algorithmical perspective.

Above all, we benefited from the book by Lichtenberg [17], which diligently uses Young tableaux for the representation theory of $SU(N)$. For Gelfand-Tsetlin patterns, the review paper by Louck [5] and Ch. 10 of the book by Barut and Rączka [18] have been the most helpful resources. Finally, there is a rather new book by Louck [19] which seems promising.

3.1 The Lie algebra $\mathfrak{su}(N)$

Let E^{pq} be the single-entry matrices, i.e. $E_{rs}^{pq} = \delta_{pr}\delta_{qs}$. One possible choice of basis of $\mathfrak{su}(N)$ is given by $i(E^{kl} + E^{lk})$ ($1 \leq k < l \leq n$), $(E^{kl} - E^{lk})$ ($1 \leq k < l \leq n$), and $i(E^{kk} - E^{k+1,k+1})$ ($1 \leq k < n$) (note the analogy to the Pauli matrices). We immediately allow complex linear combinations, thus losing anti-Hermiticity. Now define:

$$J_z^{(k)} = \frac{1}{2}(E^{kk} - E^{k+1,k+1}) \quad (1 \leq k < n), \quad (3.1)$$

$$J_+^{(k)} = E^{k,k+1} \quad (1 \leq k < n), \quad (3.2)$$

$$J_-^{(k)} = E^{k+1,k} \quad (1 \leq k < n). \quad (3.3)$$

For fixed k , these fulfill familiar-looking commutation relations:

$$\left[J_z^{(k)}, J_{\pm}^{(k)} \right] = \pm J_{\pm}^{(k)}, \quad (3.4)$$

$$\left[J_+^{(k)}, J_-^{(k)} \right] = 2J_z^{(k)}. \quad (3.5)$$

Assuredly, the operator $J_{\pm}^{(k)}$ are raising and lowering operators, in analogy to J_{\pm} known from $SU(2)$ [17, ch. 5] [7, ch. 13].

In principle, we can obtain other commutators by plugging in explicit expressions for the matrices given above, but do not need them. Furthermore, it is sufficient to focus on $J_z^{(k)}$ and $J_{\pm}^{(k)}$ instead of a full basis because, from these, we can recover a complete anti-Hermitian basis by the use of

$$E^{pq} = [J_-^{(p-1)}, [J_-^{(p-2)}, \dots [J_-^{(q+1)}, J_-^{(q)}] \dots]] \quad (p > q), \quad (3.6)$$

$$E^{pq} = [J_+^{(p)}, [J_+^{(p+1)}, \dots [J_+^{(q-2)}, J_+^{(q-1)}] \dots]] \quad (p < q). \quad (3.7)$$

We could even go as far as taking take Eqs. (3.4) to (3.7) as an abstract definition of $\mathfrak{su}(N)$. But in any case, knowing that the operators $J_z^{(k)}$ and $J_{\pm}^{(k)}$ exist and how they act on quantum states is sufficient for our purposes.

3.2 Young tableaux techniques

3.2.1 Labeling of irreps by Young diagrams

Before we proceed any further, we first need a scheme to label states in analogy to $|j, m\rangle$ in the context of angular momentum. Recall that j is a representation label and uniquely identifies an irrep of $SU(2)$. So we start by finding a labeling scheme for the irreps of $SU(N)$. It turns out that we can label each irrep of $SU(N)$ by a *Young diagram* with at most N rows [17, ch. 7] [7, ch. 16.7]. A Young diagram is an arrangement of boxes in rows and columns, such that:

1. There is a single, contiguous cluster of boxes.
2. The left borders of all rows are aligned.
3. Each row is not longer than the one above.

Note that the empty Young diagram consisting of no boxes is a valid Young diagram. For the purpose of describing an $SU(N)$ irrep, we additionally require:

4. There are at most N rows.
5. Columns with N boxes can be dropped, i.e. we identify diagrams which differ only by such columns.

Some $SU(3)$ examples are shown in Fig. 3.1. A further example is given by the Young diagrams specifying $SU(2)$ irreps: The irrep specified by total angular momentum j corresponds to a Young diagram with $2j$ boxes in a single row.

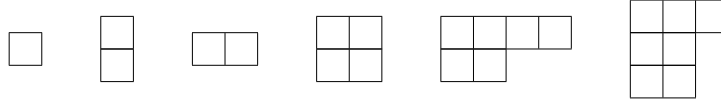


Figure 3.1. Examples of Young diagrams of $SU(3)$ irreps. As we can delete columns with 3 boxes, the last example is effectively equal to the first one.

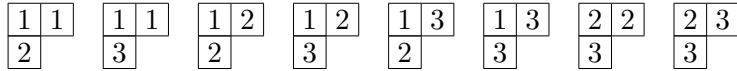


Figure 3.2. Set of all of valid $SU(3)$ Young tableaux which have the shape $\begin{array}{|c|c|} \hline \square & \square \\ \hline \square & \\ \hline \end{array}$.

As before, a given Young diagram does not uniquely identify a carrier space. Instead, the Young diagram indicates that its elements transform in a certain way under the action of the $SU(N)$ generators. Yet we often identify irreps with Young diagrams, leaving the actual carrier space to be inferred from the context.

3.2.2 Labeling of states by Young tableaux

Now that we know the generalization of the representation label j of $SU(2)$ to $SU(N)$, we also need a labeling scheme for the elements of a carrier space, corresponding to a generalization of the internal label m of $SU(2)$ irreps. This is accomplished by *semi-standard Young tableaux* [17, ch. 7], to be called, in short, Young tableaux below. A Young tableau is a Young diagram the boxes of which are filled according to the following rules:

1. Each box contains a single integer between 1 and N , inclusive.
2. The numbers in each row of boxes are weakly increasing from left to right (i.e. each number is equal to or larger than the one to its left).
3. The numbers in each column are strictly increasing from top to bottom (i.e. each number is strictly larger than the one above it).

For example, all eight Young tableaux for the diagram $\begin{array}{|c|c|} \hline \square & \square \\ \hline \square & \\ \hline \end{array}$ with respect to $SU(3)$ are shown in Fig. 3.2. As another example, let us give the correspondence between states $|jm\rangle$ of an $SU(2)$ irrep and Young tableaux: $|jm\rangle$ corresponds to a Young tableau with $2j$ boxes in a single row, of which the leftmost $j+m$ boxes contain a one and the remaining $j-m$ boxes contain a two.

Note that the dimension of a carrier space labeled by a Young diagram is given by the number of valid Young tableaux with the same shape as the Young diagram.

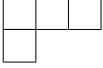
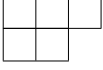
(empty)	1		8
	3		10
	3		10
	6		15
	6		15

Table 3.1. Young diagrams corresponding to the smallest $SU(3)$ irreps, along with their dimension.

3.2.3 Dimension of irreps

There exists a convenient way of calculating the dimension of an irrep given by a Young diagram [17, p. 112]. Let us consider the diagram  as an $SU(3)$ representation. First, put into each each box the number N plus the number of boxes in the same row to the left minus the number of boxes in the same column above:

$$\begin{array}{|c|c|c|c|} \hline 3 & 4 & 5 & 6 \\ \hline 2 & 3 & & \\ \hline \end{array} \quad (3.8)$$

Take the product of all these numbers, which is 2160 in this case. Then, start again and put into each box the number of boxes in the same row to the right plus the number of boxes in the same column below plus one:

$$\begin{array}{|c|c|c|c|} \hline 5 & 4 & 2 & 1 \\ \hline 2 & 1 & & \\ \hline \end{array} \quad (3.9)$$

Again, take the product which is 80 this time. The dimension is given by the former product divided by the latter, which is 27 in this case. As another example: The diagram  stands for an 8-dimensional $SU(3)$ irrep, but also for a 20-dimensional $SU(4)$ irrep. The Young diagrams corresponding to the ten smallest $SU(3)$ irreps are shown in Table 3.1.

3.2.4 Irrep product decomposition

When coupling two irreducible representations, the question arises which kind of irreps occur in their decomposition into a direct sum. The answer to this question

can be found using an easily stated but hard to prove method [20, 21].

Start with the two Young diagrams representing the two irreps to be coupled and call these the first and second diagram, respectively. The method involves writing down all possible Young tableaux for the second diagram, and using each of these to construct, starting from the first Young diagram, a new Young diagram. The set of all valid Young diagrams so produced represents the desired set of all irreps in the decomposition of the direct product. Specifically, this is done as follows:

1. Draw all admissible Young tableaux for the second diagram by filling the latter with numbers between 1 and N , inclusive, while respecting the rules for Young tableaux (weakly increasing rows, strictly increasing columns).
2. For each of these tableaux (to be called the *current Young tableau* below), construct a corresponding Young diagram, which we shall call the *trial diagram*, in the following manner:
 - a) Start the trial diagram as a fresh copy of the first diagram.
 - b) Step through the boxes of the current Young tableau from right to left, from top to bottom (in the so-called *Arabic reading order*).
 - c) If the box encountered at a given step contains the number k , add a box at the right end of row k of the trial diagram.
 - d) If this produces a trial diagram that is no longer a valid Young diagram (having a row longer than the one above), discard it and start anew with the next Young tableau.
 - e) If, however, a valid Young diagram is constructed during each step, the final Young diagram obtained after the last step represents an irrep occurring in the decomposition of the direct product.
3. The set of all trial diagrams which have not been discarded represents the desired set of all irreps in the decomposition of the direct product. If the outer multiplicity of a particular target irrep is greater than one, it will appear as many times in the set of trial diagrams.

We would like to emphasize that, after *each* step during the construction of the trial diagram, the latter has to be a valid Young diagram. Furthermore, this algorithm delivers the same result with the first and second diagram interchanged, so it requires less effort to put the smaller diagram (in the sense of the dimension of the corresponding irrep) second.

Let us illustrate the whole procedure with a simple $SU(3)$ example, the decomposition of $\begin{array}{|c|c|} \hline \square & \square \\ \hline \end{array} \otimes \begin{array}{|c|} \hline \square \\ \hline \end{array}$. Table 3.2 lists all Young tableaux for the second diagram and their corresponding trial diagrams. The Young diagrams in the rightmost column are

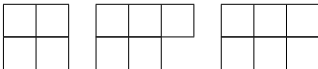
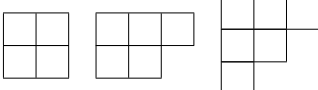
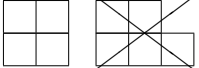
Young tableau	Construction steps of trial diagram	Final diagram
$\begin{array}{ c } \hline 1 \\ \hline 2 \\ \hline \end{array}$		
$\begin{array}{ c } \hline 1 \\ \hline 3 \\ \hline \end{array}$		
$\begin{array}{ c } \hline 2 \\ \hline 3 \\ \hline \end{array}$		discarded

Table 3.2. Steps during the $SU(3)$ decomposition of $\begin{array}{|c|} \hline \square \\ \hline \square \\ \hline \end{array} \otimes \begin{array}{|c|} \hline \square \\ \hline \end{array}$.

those which appear in the decomposition. Usually, we write this as an equation:

$$\begin{array}{|c|} \hline \square \\ \hline \square \\ \hline \end{array} \otimes \begin{array}{|c|} \hline \square \\ \hline \end{array} = \begin{array}{|c|c|c|} \hline \square & \square & \square \\ \hline \square & \square & \square \\ \hline \end{array} \oplus \begin{array}{|c|c|c|} \hline \square & \square & \square \\ \hline \square & \square & \square \\ \hline \square & & \square \\ \hline \end{array} \quad (3.10)$$

Note that we could drop the first column in the last term of Eq. 3.10, but if we retain it, all Young diagrams on the right-hand side retain the same number of boxes.

As the dimension of a product representation is the product of the dimensions of its factors, we can rewrite this equation in terms of dimensions:

$$6 \times 3 = 10 + 8 \quad (3.11)$$

This provides a simple consistency check for the decomposition.

Note that the notations used above do not reveal which $SU(N)$ the decomposition is done. If we redo the previous decomposition with respect to $SU(4)$ instead of $SU(3)$, we obtain an additional term compared to Eq. 3.10, as can be seen from Table 3.3:

$$\begin{array}{|c|} \hline \square \\ \hline \square \\ \hline \end{array} \otimes \begin{array}{|c|} \hline \square \\ \hline \end{array} = \begin{array}{|c|c|c|} \hline \square & \square & \square \\ \hline \square & \square & \square \\ \hline \end{array} \oplus \begin{array}{|c|c|c|} \hline \square & \square & \square \\ \hline \square & \square & \square \\ \hline \square & & \square \\ \hline \end{array} \oplus \begin{array}{|c|c|} \hline \square & \square \\ \hline \end{array} \quad (SU(4)) \quad (3.12)$$

Dimension-wise, this reads:

$$20 \times 6 = 50 + 64 + 6 \quad (3.13)$$

In general, we observe that, if we raise N , further terms may arise in the decomposition of a $SU(N)$ product representation.

Young tableau	Construction steps of trial diagram	Final diagram
$\begin{array}{ c } \hline 1 \\ \hline 4 \\ \hline \end{array}$		discarded
$\begin{array}{ c } \hline 2 \\ \hline 4 \\ \hline \end{array}$		discarded
$\begin{array}{ c } \hline 3 \\ \hline 4 \\ \hline \end{array}$		

Table 3.3. Additional steps during the SU(4) decomposition of $\begin{array}{|c|} \hline \square \\ \hline \square \\ \hline \end{array} \otimes \begin{array}{|c|} \hline \square \\ \hline \square \\ \hline \end{array}$ (relative to Table 3.2).

Let us consider another SU(3) example, the decomposition of $\begin{array}{|c|} \hline \square \\ \hline \square \\ \hline \end{array} \otimes \begin{array}{|c|} \hline \square \\ \hline \square \\ \hline \end{array}$, the intermediate steps of which are shown in Table 3.4:

$$\begin{array}{|c|} \hline \square \\ \hline \square \\ \hline \end{array} \otimes \begin{array}{|c|} \hline \square \\ \hline \square \\ \hline \end{array} = \begin{array}{|c|c|c|c|} \hline \square & \square & \square & \square \\ \hline \square & \square & \square & \square \\ \hline \end{array} \oplus \begin{array}{|c|c|c|} \hline \square & \square & \square \\ \hline \square & \square & \square \\ \hline \end{array} \oplus \begin{array}{|c|c|c|} \hline \square & \square & \square \\ \hline \square & \square & \square \\ \hline \end{array} \oplus \begin{array}{|c|c|c|} \hline \square & \square & \square \\ \hline \square & \square & \square \\ \hline \end{array} \oplus \begin{array}{|c|c|c|} \hline \square & \square & \square \\ \hline \square & \square & \square \\ \hline \end{array} \oplus \begin{array}{|c|c|c|} \hline \square & \square & \square \\ \hline \square & \square & \square \\ \hline \end{array} \quad (3.14)$$

Here, one term on the right-hand side appears *twice*, implying its outer multiplicity is 2, which is something that does not happen with SU(2). Recall that the decomposition of two coupled spins always leads to $j_1 \otimes j_2 = (j_1 + j_2) \oplus (j_1 + j_2 - 1) \oplus \dots \oplus |j_1 - j_2|$, where no term occurs more than once in the sum, implying each has outer multiplicity 1.

3.3 Gelfand-Tsetlin patterns

3.3.1 Correspondence to Young tableaux

The labeling of SU(N) irreps by Young diagrams and states by Young tableaux can be combined into so-called *Gelfand-Tsetlin patterns* [5, 19]. A Gelfand-Tsetlin pattern for SU(N) is a triangular arrangement of non-negative integer numbers in N rows:

$$\begin{pmatrix} m_{1N} & m_{2N} & \dots & m_{NN} \\ m_{1,N-1} & \dots & m_{N-1,N-1} & \\ \ddots & & \ddots & \\ m_{12} & m_{22} & & \\ m_{11} & & & \end{pmatrix} \quad (3.15)$$

Young tableau	Construction steps of trial diagram				Final diagram
$\begin{array}{ c c } \hline 1 & 1 \\ \hline 2 & \\ \hline \end{array}$					
$\begin{array}{ c c } \hline 1 & 1 \\ \hline 3 & \\ \hline \end{array}$					
$\begin{array}{ c c } \hline 1 & 2 \\ \hline 2 & \\ \hline \end{array}$					
$\begin{array}{ c c } \hline 1 & 2 \\ \hline 3 & \\ \hline \end{array}$					
$\begin{array}{ c c } \hline 1 & 3 \\ \hline 2 & \\ \hline \end{array}$					
$\begin{array}{ c c } \hline 1 & 3 \\ \hline 3 & \\ \hline \end{array}$					discarded
$\begin{array}{ c c } \hline 2 & 2 \\ \hline 3 & \\ \hline \end{array}$					discarded
$\begin{array}{ c c } \hline 2 & 3 \\ \hline 3 & \\ \hline \end{array}$					

Table 3.4. Steps during the $SU(3)$ decomposition of $\begin{array}{|c|c|} \hline \square & \square \\ \hline \square & \\ \hline \end{array} \otimes \begin{array}{|c|c|} \hline \square & \square \\ \hline \square & \\ \hline \end{array}$

Diagonal 1	Diagonal 2	Diagonal 3	Diagonal 4
$\begin{pmatrix} 4 \\ 3 \\ 3 \\ 2 \end{pmatrix}$	$\begin{pmatrix} 4 & 3 \\ 3 & 2 \\ 3 & 2 \\ 2 \end{pmatrix}$	$\begin{pmatrix} 4 & 3 & 1 \\ 3 & 2 & 1 \\ 3 & 2 \\ 2 \end{pmatrix}$	$\begin{pmatrix} 4 & 3 & 1 & 0 \\ 3 & 2 & 1 \\ 3 & 2 \\ 2 \end{pmatrix}$
$\begin{array}{ c c c c } \hline 1 & 1 & 2 & 4 \\ \hline \end{array}$	$\begin{array}{ c c c c } \hline 1 & 1 & 2 & 4 \\ \hline 2 & 2 & 4 & \\ \hline \end{array}$	$\begin{array}{ c c c c } \hline 1 & 1 & 2 & 4 \\ \hline 2 & 2 & 4 & \\ \hline 3 & & & \\ \hline \end{array}$	$\begin{array}{ c c c c } \hline 1 & 1 & 2 & 4 \\ \hline 2 & 2 & 4 & \\ \hline 3 & & & \\ \hline \end{array}$

Table 3.6. Alternative conversion of an $SU(4)$ Gelfand-Tsetlin pattern to a Young tableau.

fixes an irrep by specifying the number of boxes in the rows of the corresponding Young diagram. The procedure should be clear after going through the example in Table 3.5.

There is an alternative, completely equivalent way of constructing the Young tableau corresponding to a Gelfand-Tsetlin pattern, whereby the entries m_{kl} of the k -th diagonal (from left to right) of the latter are used to construct the k -th row (from top to bottom) of the former. Again, start with an empty Young tableau (no boxes at all), but proceed along the diagonals of the pattern (entries with fixed first index), from left to right (from diagonal 1 to diagonal n).

1. For a given diagonal (say the k -th), add a new, empty row (it will be the k -th row) to the bottom of the Young tableau constructed up to now.
2. Proceed upward, from bottom to top, along the entries of this k -th diagonal.
3. For each new pattern entry encountered while proceeding upwards along the diagonal (entry m_{kl} will be found in row l of the pattern), add empty boxes at the right of the k -th tableau row, to extend its length to the value of pattern entry m_{kl} .
4. Fill the newly added empty boxes in the Young tableau with the row number l of the present pattern entry.

A short demonstration is given in Table 3.6. We prefer this method when adapting the algorithm for decomposing a product representation to work on Gelfand-Tsetlin patterns. Filling a tableau in Arabic reading order corresponds to filling a pattern diagonal-wise, while adding a box to a diagram is simply done by increasing an entry in the top row of a pattern.

Generally, Gelfand-Tsetlin patterns lend themselves well to implementing on a computer the methods described in this thesis. They can be represented by much simpler data structures than Young tableaux. Another advantage is a simple formula to compute the dimension d of an irrep [18, p. 283]:

$$d = \prod_{1 \leq k < l \leq N} \left(1 + \frac{m_{kN} - m_{lN}}{l - k} \right) \quad (3.17)$$

Note that this expression depends only on the top row of a pattern. This formula gives the same result as the method described earlier involving Young diagrams.

3.3.2 Matrix elements of operators

We are now ready for explicit expressions for the action of the $J_z^{(k)}$ and $J_{\pm}^{(k)}$ operators on states labeled by Gelfand-Tsetlin patterns [18, p. 280]. In this section, denote by E^{pq} single-entry patterns, $E_{rs}^{pq} = \delta_{pr} \delta_{qs}$. For purposes of notation, define an element-wise addition and subtraction on patterns. Let M be a Gelfand-Tsetlin pattern with entries m_{kl} . The only possible non-zero matrix elements of $J_-^{(k)}$ are, for arbitrary $1 \leq j \leq k$, given by:

$$\begin{aligned} & \langle M - E^{jk} | J_-^{(k)} | M \rangle \\ &= \left(\frac{\prod_{l=1}^{k+1} (m_{l,k+1} - m_{j,k} + j - l + 1) \prod_{l=1}^{k-1} (m_{l,k-1} - m_{j,k} + j - l)}{\prod_{\substack{l=1 \\ l \neq j}}^k (m_{l,k} - m_{j,k} + j - l + 1)(m_{l,k} - m_{j,k} + j - l)} \right)^{\frac{1}{2}} \end{aligned} \quad (3.18)$$

The term $M - E^{jk}$ on the left-hand side might not be a valid pattern, but in this case, the expression above vanishes anyway. Additionally, these matrix elements are real.

As $J_+^{(k)}$ is the Hermitian transpose of $J_-^{(k)}$, we can obtain its matrix elements by taking the complex conjugate of the preceding formula ($1 \leq j \leq k$) and carefully replacing M by $M + E^{jk}$:

$$\begin{aligned} & \langle M + E^{jk} | J_+^{(k)} | M \rangle \\ &= \left(\frac{\prod_{l=1}^{k+1} (m_{l,k+1} - m_{j,k} + j - l) \prod_{l=1}^{k-1} (m_{l,k-1} - m_{j,k} + j - l - 1)}{\prod_{\substack{l=1 \\ l \neq j}}^k (m_{l,k} - m_{j,k} + j - l)(m_{l,k} - m_{j,k} + j - l - 1)} \right)^{\frac{1}{2}} \end{aligned} \quad (3.19)$$

Once again, this expression vanishes for invalid patterns $M + E^{jk}$, and all other matrix elements which do not have this form are zero.

These formulae are a generalization of Eq. (2.5). What remains is the corresponding expression for Eq. (2.4):

$$\langle M | J_z^{(k)} | M \rangle = \sum_{l=1}^k m_{l,k} - \frac{1}{2} \sum_{l=1}^{k+1} m_{l,k+1} - \frac{1}{2} \sum_{l=1}^{k-1} m_{l,k-1} \quad (3.20)$$

That is, $J_z^{(k)}$ is diagonal, and states labeled by Gelfand-Tsetlin patterns are eigenstates. Another way to obtain the last result, which might prove useful numerically, would be to evaluate the commutator $[J_+^{(k)}, J_-^{(k)}] = 2J_z^{(k)}$.

3.4 Weights

3.4.1 Weight diagrams

We define the *weight of a Young tableau*, which labels a state of an $SU(N)$ irrep, as a tuple (w_1, \dots, w_N) where w_j is the number of occurrences of j in the Young tableau. For example, the weight of $\begin{array}{|c|c|c|} \hline 1 & 1 & 1 \\ \hline 2 & 3 & \\ \hline \end{array}$ is $(3, 1, 2)$ with respect to $SU(3)$ and $(3, 1, 2, 0)$ with respect to $SU(4)$. In terms of Gelfand-Tsetlin patterns, w_j is given by the differences of row sums,

$$w_j = \sum_{i=1}^j m_{ij} - \sum_{i=1}^{j-1} m_{i,j-1}, \quad (3.21)$$

where the second sum vanishes in the case $j = 1$.

In contrast, in the literature, the weight is often defined as an $N - 1$ -tuple of the eigenvalues of a state $|M\rangle$ with respect to $J_z^{(k)}$. That is, if $J_z^{(k)} |M\rangle = \lambda_k |M\rangle$ for $1 \leq k < n$, the weight of $|M\rangle$ is $(\lambda_1, \dots, \lambda_{n-1})$. To avoid confusion of these differing definitions, we shall call the latter the *weight of a state*. However, the definitions are completely equivalent because the weight of a Young tableau determines the weight of the corresponding state and vice versa.

The weight of a state can be visualized as a vector in $N - 1$ -dimensional space. Drawing all the weights of the states of an irrep into a single $(N - 1)$ -dimensional lattice is called a *weight diagram*. For $SU(2)$, these simply consist of equidistant marks on a line, e.g. the weight diagram of the spin 2 irrep is shown in Fig. 2.1.

The weight diagrams of $SU(3)$ are two-dimensional. For example, the weights of the irrep $\begin{array}{|c|c|} \hline & \\ \hline & \\ \hline \end{array}$ are shown in Fig. 3.3. The number of distinct states having the same weight is called the *inner multiplicity* of the weight. The double circle around the weight $(0, 0)$ indicates that its inner multiplicity is 2. As a side note, some

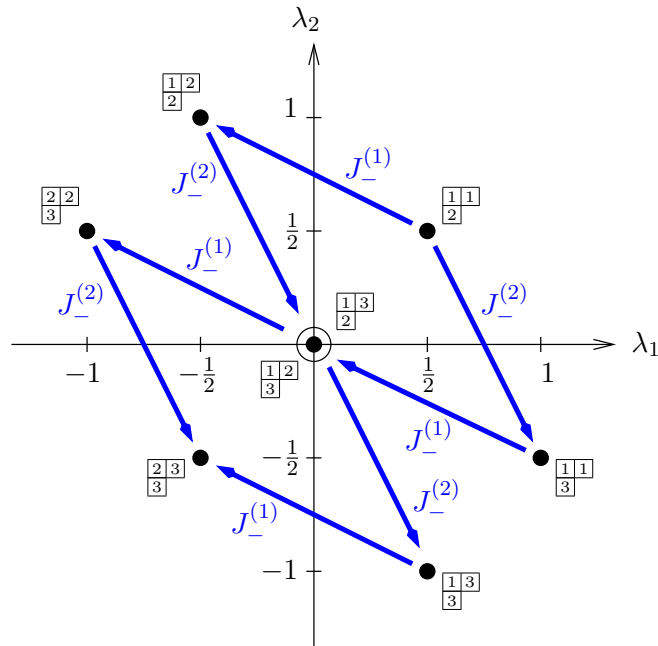


Figure 3.3. $SU(3)$ weight diagram of $\begin{smallmatrix} \square & \square \\ \square & \square \end{smallmatrix}$. Each dot represents a state, and the circle around the weight $(0,0)$ indicates that there are two states with this weight. The arrows represent the action of the $J_-^{(k)}$ operators. (The operators $J_+^{(k)}$ could be represented by arrows pointing in opposite directions to those of $J_-^{(k)}$.) $J_-^{(1)}$ acting on the state $\begin{smallmatrix} \square & \square \\ \square & \square \end{smallmatrix}$ as well as the operator $J_-^{(2)}$ acting on the state $\begin{smallmatrix} \square & \square \\ \square & \square \end{smallmatrix}$ generate linear combinations of the states $\begin{smallmatrix} \square & \square \\ \square & \square \end{smallmatrix}$ and $\begin{smallmatrix} \square & \square \\ \square & \square \end{smallmatrix}$, albeit different ones.

authors use different normalization conventions, so the weight diagrams become more symmetric.

Fig. 3.3 also illustrates the action of the lowering operators $J_-^{(k)}$. For $SU(2)$, there is only one direction in which the ladder operators can shift, but for $SU(3)$ there are two directions, so there are two raising and two lowering operators. Furthermore, it is interesting to note that the operator $J_-^{(1)}$ acting on the state $\begin{smallmatrix} \square & \square \\ \square & \square \end{smallmatrix}$ and $J_-^{(2)}$ acting on the state $\begin{smallmatrix} \square & \square \\ \square & \square \end{smallmatrix}$ generate two different linear combinations of the states $\begin{smallmatrix} \square & \square \\ \square & \square \end{smallmatrix}$ and $\begin{smallmatrix} \square & \square \\ \square & \square \end{smallmatrix}$, which are states with identical weight. For $SU(N)$, this generalizes to the following: $J_\pm^{(k)}$, when acting on a state whose Gelfand-Tsetlin pattern has weight (w_1, \dots, w_N) , produces a linear combination of all states with weight $(w_1, \dots, w_k \pm 1, w_{k+1} \mp 1, \dots, w_N)$. However, if there are no states with this

weight, the result will vanish.

For $N > 3$, the weight diagrams of $SU(N)$ cannot easily be visualized because the corresponding lattices are higher than 2-dimensional. Nevertheless, each of the ladder operators $J_{\pm}^{(k)}$ shifts in another of the $N - 1$ dimensions of the weight diagram.

3.4.2 Selection rule

In analogy to $SU(2)$, there also exists a selection rule for $SU(N)$ Clebsch-Gordan coefficients, namely the weight of a tensor product of two states is given by the element-wise sum of the individual weights of the states,

$$(w_1^M, \dots, w_{N-1}^M) = (w_1^{M_1} + w_1^{M_2}, \dots, w_{N-1}^{M_1} + w_{N-1}^{M_2}), \quad (3.22)$$

where $(w_1^M, \dots, w_{N-1}^M)$ denotes the weight of the state $|M\rangle$ and so on. Consequently, a Clebsch-Gordan coefficient between two coupled states $|M_1\rangle$ and $|M_2\rangle$ and a state of a target irrep $|M\rangle$ vanishes unless the weights add up correctly.

3.4.3 Highest-weight states

As for $SU(2)$, each $SU(N)$ irrep has a unique *highest-weight state*, which is annihilated by all $J_{+}^{(k)}$ operators for $k = 1, \dots, N - 1$ simultaneously. The highest-weight state is labeled by the Young tableau with the lowest possible entries, e.g. the highest-weight state of the $SU(3)$ irrep $\begin{array}{|c|} \hline \square \\ \hline \end{array}$ is labeled by $\begin{array}{|c|} \hline \frac{1}{2} \\ \hline \end{array}$. In terms of Gelfand-Tsetlin patterns, the pattern of the highest-weight state has the highest possible entries fulfilling the betweenness condition, i.e. $m_{kl} = m_{k,N}$ for $l < N$. The weight of the highest-weight state always has unit inner multiplicity.

In the further process of decomposing a product representation, we want to find the highest-weight states of each irrep occurring in the decomposition of the tensor product basis. For this purpose, we first find by simple inspection all product states which have the same weight as the highest-weight state of the target irrep. Let q be the number of such states, and denote them by $|M_p \otimes M'_p\rangle$, with p ranging from 1 to q . Then we need to construct all linearly independent linear combinations of these states,

$$|H_r\rangle = \sum_{p=1}^q c_p^r |M_p \otimes M'_p\rangle, \quad (3.23)$$

that satisfy the defining condition for a highest-weight state, namely that they are annihilated by all $J_{+}^{(k)}$ operators,

$$\left(J_{+}^{(k)} \otimes \mathbf{1} + \mathbf{1} \otimes J_{+}^{(k)} \right) |H_r\rangle = 0 \quad (k = 1, \dots, N - 1). \quad (3.24)$$

We can explicitly write down the action of the raising operator $J_+^{(k)}$ on the states $|M_p \otimes M'_p\rangle$ in this equation, using the matrix elements given in Eq. (3.19). This might be inconvenient on paper, but it is no problem to have a computer do this. In analogy to Eq. (2.11), we then obtain a linear system in the coefficients c_p , which are the Clebsch-Gordan coefficients of the highest-weight state of the target irrep.

3.4.4 Clebsch-Gordan coefficients with outer multiplicity

Let s denote the dimension of the null space of Eq. (3.24), i.e. the number of its independent solutions $|H_r\rangle$, $r = 1, \dots, s$. Then s gives the number of times the target irrep occurs in the decomposition of the direct product, i.e. it is the *outer multiplicity* of the target irrep. (It coincides with the outer multiplicity obtained by the Young tableaux method of Sec. 3.2.4.) An outer multiplicity larger than 1 leads to an ambiguity among the Clebsch-Gordan coefficients of the highest-weight states of target irreps of the same kind, as the set of highest-weight states is not uniquely defined: a unitary transformation $|H_r\rangle \rightarrow \sum_{r'} U_{rr'} |H'_r\rangle$ among this set will produce a different (but equally acceptable) set of highest weight states. The full set of Clebsch-Gordan coefficients of these target irreps will change accordingly.

We are not aware of a canonical resolution of this ambiguity, i.e. a way of resolving it using group theoretical considerations (although we suspect that this might be possible using Casimir operators). However, we suggest writing down the independent solutions, (c_1^r, \dots, c_q^r) , where $r = 1, \dots, s$ indexes the solutions and s is the outer multiplicity, as a matrix,

$$\begin{pmatrix} c_1^1 & \cdots & c_q^1 \\ \vdots & \ddots & \vdots \\ c_1^s & \cdots & c_q^s \end{pmatrix}, \quad (3.25)$$

and bringing this matrix into reduced row echelon form by Gaussian elimination [22]. The resulting matrix will be of the form

$$\begin{pmatrix} 0 & \cdots & 0 & + & 0 & \cdots & 0 & 0 & 0 & \cdots & 0 & 0 & * & \cdots & * \\ 0 & \cdots & 0 & 0 & 0 & \cdots & 0 & + & 0 & \cdots & 0 & 0 & * & \cdots & * \\ 0 & \cdots & 0 & 0 & 0 & \cdots & 0 & 0 & 0 & \cdots & 0 & 0 & * & \cdots & * \\ \vdots & \ddots & \vdots & \vdots & \vdots & \ddots & \vdots & \vdots & \vdots & \ddots & \vdots & \vdots & \vdots & \ddots & \vdots \\ 0 & \cdots & 0 & 0 & 0 & \cdots & 0 & 0 & 0 & \cdots & 0 & 0 & * & \cdots & * \\ 0 & \cdots & 0 & 0 & 0 & \cdots & 0 & 0 & 0 & \cdots & 0 & + & * & \cdots & * \end{pmatrix}, \quad (3.26)$$

where $+$ and $*$ denote positive and arbitrary matrix elements, respectively. This normal form is the same for all equivalent matrices. However, the resulting highest-weight states might not be orthonormal, so a further orthogonalization process is required. If carefully specified in which order this orthogonalization is done, the resulting Clebsch-Gordan coefficients of the highest-weight states will be unique.

3.5 Generating lower-weight states of an irrep

After we have generated the Clebsch-Gordan coefficients of the highest-weight state of a particular target irrep, we can go on to calculating the Clebsch-Gordan coefficients of the other states of this irrep. In general terms, this is accomplished by repeatedly acting on both sides of Eq. (3.23) with the lowering operators $J_-^{(k)}$. On the left hand side, we act on the kets by the matrix representing a given $J_-^{(k)}$ in target irrep, and on the right hand side we use the matrix representing $J_-^{(k)}$ in the product representation of the coupled carrier spaces.

Let us repeat how the lowering operators act on a state $|M\rangle$ labeled by a given Gelfand-Tsetlin pattern (see Sec. 3.4.1). If (w_1, \dots, w_N) is the weight of a state M , then $J_-^{(k)}|M\rangle$ produces a linear combination of all states with weight $(w_1, \dots, w_k + 1, w_{k+1} - 1, \dots, w_N)$. If there are no states with the latter weight, the result vanishes. Because we cannot reach each state with a given weight from the highest-weight state independently (only linear combinations of them), we cannot determine the Clebsch-Gordan coefficients of the states with this weight independently. However, when there are multiple states with the same weight, say t of them, there always are as many “parent states”, i.e. states which generate a linear combination of those t states when acted upon by the proper lowering operator.

Thus, when we have determined the Clebsch-Gordan of a highest-weight state $|H_r\rangle$, we act on Eq. (3.23) by $J_-^{(1)}$, $J_-^{(2)}$, and so on to $J_-^{(N-1)}$. Each of the resulting equations will determine the Clebsch-Gordan coefficients for a further state. Let $(w_1^{H_r}, \dots, w_N^{H_r})$ stand for the weight of the Gelfand-Tsetlin pattern H_r . Then we can, for example, act with $J_-^{(1)}J_-^{(2)}$ as well as $J_-^{(2)}J_-^{(1)}$ on Eq. (3.23), which results in two equations for the states with weight $(w_1^{H_r} - 1, w_2^{H_r}, w_3^{H_r} + 1, w_4^{H_r}, \dots, w_N^{H_r})$. Remarkably, it turns out that there are never more states with identical weight than we can obtain equations in their Clebsch-Gordan coefficients.

Formally, if there are t states, say $|L_1\rangle, \dots, |L_t\rangle$, which have identical weight (w_1^L, \dots, w_N^L) , and if there are u states $|M_1 \otimes M'_1\rangle, \dots, |M_u \otimes M'_u\rangle$ in the old basis which also possess this weight, we always obtain at least t linearly independent equations of the form

$$\sum_{t'=1}^t \gamma_{t'}^v |L_{t'}\rangle = \sum_{u'=1}^u c_{u'}^v |M_{u'} \otimes M'_{u'}\rangle \quad (v = 1, \dots, t). \quad (3.27)$$

Here, v enumerates the various equations, $\gamma_{t'}$ are the coefficients of a linear combination of the states $|L_1\rangle, \dots, |L_t\rangle$, and $c_{u'}^v$ are some coefficients which are not Clebsch-Gordan coefficients yet. However, Eq. (3.27) presents a system of equations which can be solved for the Clebsch-Gordan coefficients of the states $|L_1\rangle, \dots, |L_t\rangle$.

Let us repeat that the system of equations (3.27) is obtained by acting with the

lowering operators $J_-^{(k)}$ on the corresponding equations for the states with weight $(w_1^L, \dots, w_k^L - 1, w_{k+1}^L + 1, \dots, w_N^L)$. In turn, the Clebsch-Gordan coefficients of these states have to have been determined prior to that. In general, the Clebsch-Gordan coefficients of a target irrep are determined weight by weight, starting from the highest weight and sweeping over the whole weight diagram. In other words, we obtain the Clebsch-Gordan coefficients of the lower-weight states in a cascade-like manner: First the highest-weight state, then all states with a weight one level below the highest weight, and so on.

3.6 Construction of all Clebsch-Gordan coefficients

3.6.1 Review of the algorithm

We now have all the ingredients necessary to compute the full set of $SU(N)$ Clebsch-Gordan coefficients, defined as the unitary matrix C which brings the matrices of the generators on a tensor product space into block-diagonal form (Eq. (1.23)). Starting from two Young diagrams, perform the following steps:

1. Generate explicit matrices $\Gamma(J_{\pm}^{(k)})$ for the raising and lowering operators in the first and second irrep, using Eqs. (3.19) and (3.18). Take the appropriate Kronecker products to find the matrices acting on the tensor product space.
2. Find the irreps appearing in the decomposition, using the method described in sec. 3.2.4. For each target irrep, do the following:
 - a) Compute the highest weight of the target irrep and find all according tensor product states $|M_p \otimes M'_p\rangle$, with $p = 1, \dots, q$, say, whose weight agrees with this highest weight.
 - b) Find a maximal set of linearly independent linear combinations of the latter,

$$|H_T\rangle = \sum_p c_p^r |M_p \otimes M'_p\rangle, \quad (3.28)$$

which are simultaneously annihilated by all raising operators, as described in Eq. (3.24). The number s is the outer multiplicity of the target irrep in the decomposition. Each such linear combination defines the highest-weight state of one of the occurrences of the target irrep.

- c) Act with all non-vanishing strings of lowering operators $J_-^{(k_1)} J_-^{(k_2)} \dots$ on both sides of Eq. (3.28), using the representation appropriate for the target irrep on the left hand side, and the direct product representation on the right hand side. Group the resulting equations by the weight of the states occurring in each one, which must be the same in a single equation.

- d) For every weight of the target irrep, we now have a system of equations as in Eq. (3.27). Weight by weight, starting from the highest-weight, solve these systems of equations for the Clebsch-Gordan coefficients of the lower-weight states of the target irrep.

The notion of weights allows us to compute the Clebsch-Gordan coefficients of the lower-weight states in an efficient manner. For a given weight, there are only few states in most cases, and we obtain a system of equations in their Clebsch-Gordan coefficients independently from those of the states with different weights. Thus, it is little work to solve for the Clebsch-Gordan coefficients of the states with a given weight.

3.6.2 Consistency checks

We have undertaken the following checks, at least in a decent number of small cases, to verify that our program correctly computes Clebsch-Gordan coefficients:

- For $SU(2)$, the results coincide with the formulas given in Ch. 2, up to sign conventions.
- For $SU(3)$, some results are available in the relevant literature.
- The matrix of Clebsch-Gordan coefficients is unitary.
- The matrix of Clebsch-Gordan block-diagonalizes the representation matrices of the generators of $SU(N)$.
- The selection rule (3.22) is fulfilled.

The latter three properties are, of course, known to be true in general for Clebsch-Gordan coefficients. For our program code, they have not been used as input in constructing the code, but hold as properties of its output. These checks render us confident that our code works properly.

Chapter 4

Symmetries in the Numerical Renormalization Group

The *Numerical Renormalization Group*, or NRG, in short, was developed by Wilson in 1975 to treat the Kondo problem in a nonperturbative fashion. For the purpose of this thesis, we do not need the full machinery of NRG and thus refer to the literature for a comprehensive description. Good introductions are given in the original papers by Wilson [23, 24], the papers by Krishna-murthy [2, 25], and the review by Bulla [26]. More recent developments include spectral sum-conserving methods [27, 1], matrix product states approaches [28], and time-dependent NRG [29]. Symmetries in NRG have been considered as early as in [2, App. B], but their treatment in this thesis is mainly based on the work of Tóth et al. [3].

4.1 Structure of the Hamiltonian

The Hamiltonians to which we apply NRG share a particular form, namely that of a half-infinite quantum chain, the so-called *Wilson chain*. For example, the Hamiltonian of the single-impurity Anderson model, after the transformation to the Wilson chain, is given by [2, Eq. (2.18)]

$$\begin{aligned} H = & \tilde{H}_{\text{imp}} + T_0 \sum_m \left(f_{0,m}^\dagger d_m + \text{h.c.} \right) \\ & + \sum_{k=1}^{\infty} T_k \sum_m \left(f_{k,m}^\dagger f_{k-1,m} + \text{h.c.} \right), \end{aligned} \tag{4.1}$$

where \tilde{H}_{imp} is the local Hamiltonian of the impurity, d_m^\dagger and $f_{k,m}^\dagger$ are fermionic creation operators at the impurity and the site k of the Wilson chain, respectively, and T_0 and T_k are coupling constants. The latter have the important property of decaying exponentially along the chain, $T_k \propto \Lambda^{-k/2}$, where $\Lambda > 1$ is a so-called discretization parameter, typically chosen between 1.5 and 3.

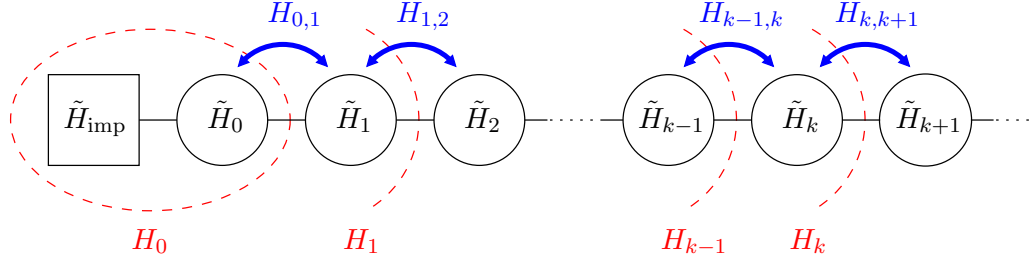


Figure 4.1. Depiction of the Wilson chain. The square box represents the impurity while the circles represent the sites of the Wilson chain. The Hamiltonian includes only local terms (denoted by \tilde{H}_k) and nearest-neighbor hopping terms (denoted by $H_{k,k+1}$).

The most general form of the Hamiltonian relevant to us is [3, Eq. (2)]

$$H = H_0 + \sum_{k=1}^{\infty} (H_{k-1,k} + \tilde{H}_k), \quad (4.2)$$

where H_0 is a local term describing the impurity and its coupling to the bath, $H_{k-1,k}$ is a hopping term between sites $k-1$ and k , and \tilde{H}_k is a local term of the site k of the Wilson chain. It is helpful to visualize this Hamiltonian as a semi-infinite discrete chain with nearest-neighbor hopping, as shown in Fig. 4.1. The Hamiltonian of Eq. (4.1) can be transformed to this form by taking

$$H_0 = \tilde{H}_{\text{imp}} + T_{\text{imp},0} \sum_m (f_{0,m}^\dagger d_m + \text{h.c.}), \quad (4.3)$$

$$H_{k-1,k} = T_k \sum_m (f_{k,m}^\dagger f_{k-1,m} + \text{h.c.}), \quad (4.4)$$

and $\tilde{H}_k = 0$. The local term \tilde{H}_k will not be present in most cases, but we still retain it for the sake of generality.

4.2 Symmetries of the Hamiltonian

Typically, each H_k will be invariant with respect to some Abelian or non-Abelian symmetry. For example, the generators \vec{S} of an SU(2) spin symmetry are given by [3, Table 1]

$$\vec{S}_k = \vec{S}_{\text{imp}} + \frac{1}{2} \sum_{k'=0}^k \sum_{m,m'} f_{k',m}^\dagger \vec{\sigma}_{m,m'} f_{k',m'}, \quad (4.5)$$

where $\vec{\sigma}$ are the Pauli matrices (Eq. (1.9)). The generator C_z of a U(1) charge symmetry is given by

$$C_z = \frac{1}{2} \sum_{k'=0}^k \sum_m (f_{k',m}^\dagger f_{k',m} - 1). \quad (4.6)$$

It is important to note that, to be able to group the states into symmetry multiplets in each NRG iteration, the Hamiltonian H_k has to commute with these generators.

We will not explicitly consider multiple symmetries, such as $SU(2) \times SU(3)$, to avoid bloated notation, but they can be taken into account by a straightforward generalization of the approach sketched below. In fact, we only have to consider the representation and internal labels as multi-indices, i.e. a single representation label j has to be replaced by $(j^{(a)}, j^{(b)})$, and an internal label m has to be replaced by a multi-index $(m^{(a)}, m^{(b)})$. Each part of such a multi-index, in turn, can represent any symmetry-specific label, such as a Young diagram or a Gelfand-Tsetlin pattern. Furthermore, a Clebsch-Gordan coefficient between states which have multi-index symmetry labels, is given by the product of the individual Clebsch-Gordan coefficients [3, after Eq. (11)], e.g.

$$\begin{aligned} & \langle j_1^{(a)} j_1^{(b)}, m_1^{(a)} m_1^{(b)}; j_2^{(a)} j_2^{(b)}, m_2^{(a)} m_2^{(b)} | j^{(a)} j^{(b)}, m^{(a)} m^{(b)} \rangle \\ &= \langle j_1^{(a)} m_1^{(a)}; j_2^{(a)} m_2^{(a)} | j^{(a)} m^{(a)} \rangle \langle j_1^{(b)} m_1^{(b)}; j_2^{(b)} m_2^{(b)} | j^{(b)} m^{(b)} \rangle. \end{aligned} \quad (4.7)$$

4.3 Statement of the algorithm

We rewrite the Hamiltonian of Eq. (4.2) as a recursion relation for $k \geq 1$ [3, Eq. (4)],

$$H_k = H_{k-1} + H_{k-1,k} + \tilde{H}_k \quad (4.8)$$

The general idea of NRG is to construct H_k from H_{k-1} and diagonalize it, successively for each $k = 0, 1, 2, \dots$. As the coupling between sites $k-1$ and k decays exponentially [2, Eq. (2.14)], the effective level spacing of H_k is of order $\Lambda^{-k/2}$, in other words, by considering ever longer chains, one resolves the eigenspectrum of the system with ever smaller resolution. The eigenvalues of the rescaled Hamiltonian $H'_k = \Lambda^{k/2}(H_k - E_{G,k})$ (where $E_{G,k}$ is the ground state energy of H_k) converge once the chain has become so long that the effective level spacing of H_k is smaller than the smallest relevant energy scale of the problem. Thus, the iterative procedure can be stopped once the chain has become sufficiently long, which typically happens for chain lengths of order 60 to 80.

Another issue is that of the dimension of the state space of H_k , which grows exponentially with the number of iterations. Therefore, after the diagonalization of

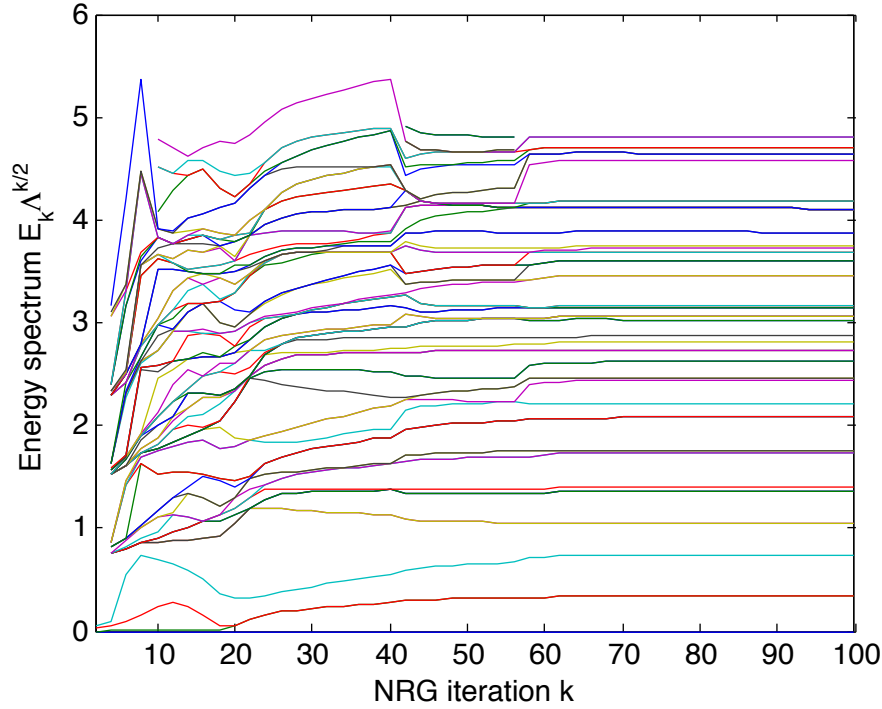


Figure 4.2. Example of an energy flow diagram for the single-impurity Anderson model. The energy spectrum of H_k is plotted against k . Λ is an energy discretization constant. The convergence of the energy spectrum is visible at later iterations.

H_k , we truncate the state space by keeping only a certain number of lowest-energy states, usually on the order of 1 000. The set of states after diagonalization is thus divided into *discarded* and *kept* states. The latter are also called *block* or *old* states.

The above steps have been standard in NRG since its original conception by Wilson in 1975. Our goal in this thesis is to describe how to perform them while respecting and exploiting arbitrary $SU(N)$ symmetries of the Hamiltonian. All in all, an NRG run consists of the following steps:

1. Diagonalize H_0 .
2. For each site of the Wilson chain, from $k = 1$ to the desired limit, repeat:
 - a) Sort the eigenstates of H_{k-1} in order of increasing eigenenergies, measured with respect to $E_{G,k-1}$. The eigenstates will fall into symmetry multiplets, each forming an irreducible representation of the symmetry group of H_{k-1} .

- b) Discard the highest-lying multiplets to truncate the state space of H_{k-1} to the desired size.
- c) Transform the creation and annihilation operators f_{k-1}^\dagger and f_{k-1} into the eigenbasis of H_{k-1} .
- d) Enlarge the state space by taking the tensor product with the local states of site k . The Hamiltonian H_{k-1} is mapped to $H_{k-1} \otimes \mathbb{1}$, the creation operators f_{k-1}^\dagger to $f_{k-1}^\dagger \otimes \mathbb{1}$ and so on.
- e) Transform the basis of the state space once again to obtain states with “good” symmetry quantum numbers, i.e. decompose the product state space into a sum of irreducible representations of the symmetry group. The matrix describing this change of basis is composed of several Clebsch-Gordan matrices. Now, also the local Hamiltonian \tilde{H}_k , if present, and the local creation annihilation operators f_k^\dagger and f_k have to be transformed into this new basis.
- f) Construct the new Hamiltonian H_k via Eq. (4.8).
- g) Diagonalize H_k .

An important outcome of an NRG run is the so-called *energy flow diagram*, on which the lowest-lying few eigenenergies of the rescaled Hamiltonian H'_k are plotted against the iteration number k . A typical example is shown in Fig. 4.2.

In the subsequent sections, we are going to discuss these steps with regard to the use of symmetries. Symmetries allow us to greatly improve upon the truncation scheme. By the use of the Wigner-Eckart theorem, we only maintain the reduced matrix elements of the Hamiltonian instead of matrix elements between all kept states. That effectively corresponds to keeping track of a single state per symmetry multiplet, thereby increasing the number of kept states by the average dimension of a multiplet, which is on the order of 5 to 10. Additionally, the diagonalization takes less time because the state space is sliced into smaller blocks, which allows a further increase in the number of kept states.

4.4 Reduced matrix elements of the initial Hamiltonian

As we would like to work only with reduced matrix elements throughout an NRG run, we have to compute the reduced matrix elements of H_0 at the beginning. This will also serve as a general example of how to determine reduced matrix elements of irreducible tensor operators.

We start by grouping the states of the Hilbert space into symmetry multiplets. As an example, let us assume that every site in Fig. 4.1 has four basis states, $|0\rangle$, $|\uparrow\rangle$, $|\downarrow\rangle$, and $|\uparrow\downarrow\rangle$, and that each H_k is invariant under spin rotations [3, Eq. (5)], which is an $SU(2)$ symmetry. Then the basis states span three invariant subspaces

	$ 0 \otimes 0\rangle$
	$ 0 \otimes \uparrow\downarrow\rangle$
$j = 0$	$ \uparrow\downarrow \otimes 0\rangle$
	$ \uparrow\downarrow \otimes \uparrow\downarrow\rangle$
	$(\uparrow \otimes \downarrow\rangle - \downarrow \otimes \uparrow\rangle)/\sqrt{2}$
	$ 0 \otimes \uparrow\rangle, 0 \otimes \downarrow\rangle$
$j = 1/2$	$ \uparrow \otimes 0\rangle, \downarrow \otimes 0\rangle$
	$ \uparrow \otimes \uparrow\downarrow\rangle, \downarrow \otimes \uparrow\downarrow\rangle$
	$ \uparrow\downarrow \otimes \uparrow\rangle, \uparrow\downarrow \otimes \downarrow\rangle$
$j = 1$	$ \uparrow \otimes \uparrow\rangle, (\uparrow \otimes \downarrow\rangle + \downarrow \otimes \uparrow\rangle)/\sqrt{2}, \downarrow \otimes \downarrow\rangle$

Table 4.1. SU(2) symmetry multiplets of the state space of H_0 . These are found by coupling the multiplets of the impurity and of the first site of the Wilson chain.

under the action of SU(2) generators, two singlets, $|0\rangle$ and $|\uparrow\downarrow\rangle$, and a doublet, $\{|\uparrow\rangle, |\downarrow\rangle\}$. However, the state space of H_0 is spanned by the tensor products of two of these states, one living on the impurity and one living on the first site of the Wilson chain, so we have to couple all impurity states with all first-site states. The resulting multiplets are shown in Table 4.1.

We see that there are five $j = 0$ multiplets, four $j = 1/2$ multiplets, and one $j = 1$ multiplet. The Hamiltonian can only have non-vanishing matrix elements between multiplets of the same kind, so instead of $16^2 = 256$ matrix elements for each pair of states, we only need $5^2 + 4^2 + 1^2 = 42$ reduced matrix elements. What remains, is to evaluate the formula given in Eq. (1.26) for each reduced matrix element.

As the Hamiltonian is a scalar operator, this formula simplifies to

$$\langle n'j || H || nj \rangle = \frac{1}{2j+1} \sum_{m'} \langle n'jm' | H | njm' \rangle \quad (4.9)$$

in the case of an SU(2) spin symmetry.

Let us give another brief example, an SU(3) color symmetry. We assume that there are not two, but three species of fermions living on the Wilson chain, which we call r, g, and b, instead of \uparrow and \downarrow . The basis states of the local state space of a single site are shown in Table 4.2. When the impurity and the first site of the Wilson chain are coupled, the state space resolves into six singlets (corresponding to an empty Young diagram), five multiplets of the type \square , five multiplets of the type \square , two multiplets of the type $\square\square$, and one multiplet of the types $\square\square$ and $\square\square$

(empty)	$ 0\rangle$
	$ \text{rgb}\rangle$
\square	$ \boxed{1}\rangle = r\rangle, \boxed{2}\rangle = g\rangle, \boxed{3}\rangle = b\rangle$
$\begin{array}{ c } \hline \square \\ \hline \square \\ \hline \end{array}$	$ \begin{array}{ c } \hline \boxed{1} \\ \hline \boxed{2} \\ \hline \end{array}\rangle = \text{rg}\rangle, \begin{array}{ c } \hline \boxed{1} \\ \hline \boxed{3} \\ \hline \end{array}\rangle = \text{rb}\rangle, \begin{array}{ c } \hline \boxed{2} \\ \hline \boxed{3} \\ \hline \end{array}\rangle = \text{gb}\rangle$

Table 4.2. SU(3) symmetry multiplets of a local state space. Irreps are labeled by Young diagrams, and states are labeled by Young tableaux.

each. The reduction in the number of matrix elements is impressive: Instead of the $64^2 = 4096$ individual matrix elements of the initial Hamiltonian, we need only $6^2 + 2 \times 5^2 + 2^2 + 2 \times 1^2 = 92$ reduced matrix elements.

4.5 Iterative construction of the Hamiltonian

After the reduced matrix elements of H_0 have been found, and the initial diagonalization has been done, the main loop of NRG starts. In each iteration, we construct the Hamiltonian H_k via Eq. (4.8). Therefore, we need the reduced matrix elements of H_{k-1} , $H_{k-1,k}$, and \tilde{H}_k .

4.5.1 Construction of states with good quantum numbers

Let us recall the setting at this stage. The state space of H_{k-1} is spanned by the block states. Besides a representation label j_{k-1} and an internal label m_{k-1} , we only need *one* additional label n_{k-1} to identify each block state uniquely. Even though we use further labels during the construction of the new states to resolve outer multiplicity ambiguities, we eventually replace these with a single integer n_{k-1} label by enumerating all states with given symmetry labels j_{k-1} and m_{k-1} sequentially. This allows us to conveniently denote the block states as $|n_{k-1}, j_{k-1}, m_{k-1}\rangle$. Apart from that, we assume that H_{k-1} has been diagonalized in the previous iteration, i.e.

$$\langle n'_{k-1}, j'_{k-1} || H_{k-1} || n_{k-1}, j_{k-1} \rangle = E_{n_{k-1}, j_{k-1}} \delta_{j'_{k-1}, j_{k-1}} \delta_{n'_{k-1}, n_{k-1}}. \quad (4.10)$$

Likewise, the state space of the local Hamiltonian \tilde{H}_k is spanned by the local states $|\tilde{n}_k, \tilde{j}_k, \tilde{m}_k\rangle$, with a representation label \tilde{j}_k , an internal label m_k , and an additional label n_k , in analogy to the block states. The reduced matrix elements of \tilde{H}_k are obtained in the same way as for H_0 , i.e. by identifying the symmetry multiplets of the local state space and evaluating Eq. (1.26).

Although we denote representation and internal labels by single letters j and m , respectively, we would like to point out that the j and m can be anything from the familiar $|jm\rangle$ of angular momentum to, e.g., a multi-index composed of a mix of Casimir operator eigenvalues and Young diagrams.

We then couple each block state multiplet with each local state multiplet and switch over to a new basis $|n_{k-1}, j_{k-1}, \tilde{n}_k, \tilde{j}_k, j, m, \alpha\rangle$ with well-defined symmetry quantum numbers j and m ,

$$\begin{aligned} & |n_{k-1}, j_{k-1}, \tilde{n}_k, \tilde{j}_k, j, m, \alpha\rangle \\ &= \sum_{m_{k-1}, \tilde{m}_k} \langle j_{k-1}, m_{k-1}; \tilde{j}_k, \tilde{m}_k | j, m, \alpha \rangle |n_{k-1}, j_{k-1}, m_{k-1}; \tilde{n}_k, \tilde{j}_k, \tilde{m}_k\rangle, \end{aligned} \quad (4.11)$$

where n_{k-1} and j_{k-1} designate the symmetry multiplet of the block states from which $|n_{k-1}, j_{k-1}, \tilde{n}_k, \tilde{j}_k, j, m, \alpha\rangle$ is constructed, \tilde{n}_k and \tilde{j}_k designate the corresponding multiplet of the local states, and α distinguishes between several occurrences of the irrep labeled by j in the decomposition of $j_{k-1} \otimes \tilde{j}_k$. The coefficient $\langle j_{k-1}, m_{k-1}; \tilde{j}_k, \tilde{m}_k | j, m, \alpha \rangle$ appearing in Eq. (4.11) is a Clebsch-Gordan coefficient.

4.5.2 Reduced matrix elements of the new Hamiltonian

The reduced matrix elements of H_{k-1} and \tilde{H}_k in the new basis have a simple form [3, Eqs. (17) and (18)], as they depend on either the block states or the local states:

$$\begin{aligned} & \langle n'_{k-1}, j'_{k-1}, \tilde{n}'_k, \tilde{j}'_k, j', \alpha' | H_{k-1} | n_{k-1}, j_{k-1}, \tilde{n}_k, \tilde{j}_k, j, \alpha \rangle \\ &= E_{n_{k-1}, j_{k-1}} \delta_{n'_{k-1}, n_{k-1}} \delta_{j'_{k-1}, j_{k-1}} \delta_{\tilde{n}'_k, \tilde{n}_k} \delta_{\tilde{j}'_k, \tilde{j}_k} \delta_{j', j} \delta_{\alpha', \alpha}, \end{aligned} \quad (4.12)$$

$$\begin{aligned} & \langle n'_{k-1}, j'_{k-1}, \tilde{n}'_k, \tilde{j}'_k, j', \alpha' | \tilde{H}_k | n_{k-1}, j_{k-1}, \tilde{n}_k, \tilde{j}_k, j, \alpha \rangle \\ &= \langle \tilde{n}'_k, \tilde{j}'_k | \tilde{H}_k | \tilde{n}_k, \tilde{j}_k \rangle \delta_{n'_{k-1}, n_{k-1}} \delta_{j'_{k-1}, j_{k-1}} \delta_{\tilde{j}'_k, \tilde{j}_k} \delta_{j', j} \delta_{\alpha', \alpha}. \end{aligned} \quad (4.13)$$

The case of the reduced matrix elements of the hopping operator $H_{k-1,k}$ is more complicated. Let us assume that $H_{k-1,k}$ can be written, apart from some prefactors, as a sum over creation/annihilation operator combinations, where the sum runs over the components of a *creation operator multiplet* [3, Eq. (19)],

$$H_{k-1,k} = \sum_m \left(f_{k,m}^\dagger f_{k-1,m} + \text{h.c.} \right). \quad (4.14)$$

Here, the creation operators $\{f_{k,m}^\dagger\}$ at site k form an irreducible tensor operator of rank N , the number of fermion species. The annihilation operators $\{f_{k-1,m}\}$ form an irreducible tensor operator as well. We can obtain (see App. B) an expression for the reduced matrix elements of $H_{k-1,k}$ which only depends on previously determined quantities (note that $H_{k-1,k}$ is, as part of the Hamiltonian, a scalar operator, and

thus the reduced matrix elements of $H_{k-1,k}$ do not depend on an outer multiplicity index, in contrast to Eq. (1.26)):

$$\begin{aligned}
& \langle n'_{k-1}, j'_{k-1}, \tilde{n}'_k, \tilde{j}'_k, j', \alpha' || H_{k-1,k} || n_{k-1}, j_{k-1}, \tilde{n}_k, \tilde{j}_k, j, \alpha \rangle \\
&= \sum_{m'} \sum_{m'_{k-1}} \sum_{\tilde{m}'_k} \sum_{m_{k-1}} \sum_{\tilde{m}_k} \sum_m \sum_{\alpha_{k-1}} \sum_{\tilde{\alpha}_k} \frac{\delta_{j',j}}{\dim j} \\
& \langle j', m', \alpha' | j'_{k-1}, m'_{k-1}; \tilde{j}'_k, \tilde{m}'_k \rangle \langle j_{k-1}, m_{k-1}; \tilde{j}_k, \tilde{m}_k | j, m', \alpha \rangle \\
& \left(\langle j_{k-1}, m_{k-1}, \alpha_{k-1} | j_f, m; j'_{k-1}, m'_{k-1} \rangle^* \langle \tilde{j}'_k, \tilde{m}'_k, \tilde{\alpha}_k | j_f, m; \tilde{j}_k, \tilde{m}_k \rangle \right. \\
& \langle n_{k-1}, j_{k-1} || f_{k-1} || n'_{k-1}, j'_{k-1} \rangle^* \langle \tilde{n}'_k, \tilde{j}'_k || f_k || \tilde{n}_k, \tilde{j}_k \rangle \\
& + \langle j'_{k-1}, m'_{k-1}, \alpha_{k-1} | j_f, m; j_{k-1}, m_{k-1} \rangle \langle \tilde{j}_k, \tilde{m}_k, \tilde{\alpha}_k | j_f, m; \tilde{j}'_k, \tilde{m}'_k \rangle^* \\
& \left. \langle n'_{k-1}, j'_{k-1} || f_{k-1} || n_{k-1}, j_{k-1} \rangle \langle \tilde{n}_k, \tilde{j}_k || f_k || \tilde{n}'_k, \tilde{j}'_k \rangle^* \right). \tag{4.15}
\end{aligned}$$

Here, j_f is the representation label of the irreducible tensor operators $\{f_{k-1,m}\}$ and $\{f_{k,m}\}$. This formula is a slight generalization of Eq. (20) from [3] as it takes into account outer multiplicities, which do not occur within SU(2).

4.5.3 Diagonalization and relabeling

After determining the reduced matrix elements of H_{k-1} , \tilde{H}_k , and $H_{k-1,k}$, the construction of the Hamiltonian H_k is complete, and we proceed to diagonalize H_k . Before we turn to the next NRG iteration, we sort states by their representation label j_k and assign each state for a given j_k a unique integer n_k . However, states with different representation label j_k may have the same label n_k . Instead of $|n_{k-1}, j_{k-1}, \tilde{n}_k, \tilde{j}_k, j, m, \alpha\rangle$, we relabel the states of the diagonal basis by $|n_k, j_k, m_k\rangle$. This relabeling establishes the prerequisites to start the next iteration at Eq. (4.10), i.e.

$$\langle n'_k, j'_k || H_k || n_k, j_k \rangle = E_{n_k, j_k} \delta_{j'_k, j_k} \delta_{n'_k, n_k}. \tag{4.16}$$

4.6 Creation operator multiplets

As seen in the previous section, our approach to symmetries in NRG relies on dealing with irreducible tensor operators. If we would like to keep track of an arbitrary operator during the NRG iterations, we first have to find all components of the irreducible tensor operator this particular operator belongs to, so we can compute its reduced matrix elements. Unfortunately, the identification of irreducible tensor operators is not a trivial task, and we do not know of a general method, at

present. However, we give some preliminary remarks which should help to construct arbitrary irreducible tensor operators.

In particular, the creation operators $\{f_m^\dagger\}, m = 1, \dots, N$, form an $SU(N)$ irreducible tensor operator, transforming as the irrep labeled by the Young diagram \square , a single box. In contrast, the annihilation operators $\{f_m\}, m = 1, \dots, N$, form an irreducible tensor operator which transforms as the irrep labeled by the Young diagram consisting of a single column with $N - 1$ boxes.

As a handwaving argument, the creation operator create a single fermion when applied to the vacuum state $|0\rangle$, which transforms into another species (or linear combination thereof) of fermions under the action of $SU(N)$ generators. This in turn corresponds to some other creation operator (or linear combination thereof) applied to the vacuum, so the creation operators must form an invariant operator subspace, which is precisely the definition of an irreducible tensor operator. Analogously, applying the annihilation operators to a fully occupied state leads to states with one fermion species missing, which transform into each other under $SU(N)$ rotations. So, the annihilation operators also form a rank- N irreducible tensor operator.

Moreover, the operator $\sum_m f_m^\dagger f_m$ is a scalar under symmetry group transformations, which results from coupling the creation operator multiplet with the annihilation operator multiplet. The only N -dimensional irreps of $SU(N)$ are given by the Young diagrams with a single box and with $N - 1$ boxes in a column, so the creation and annihilation operators have to transform as one of these irreps. Furthermore, a singlet only occurs in the decomposition of the product of the single-box diagram with the $N - 1$ -box diagram, but not in the product of the single-box diagram with itself, and not in the product of the $N - 1$ -box diagram with itself.

More rigorously [30], consider the N -dimensional irrep of $SU(N)$, and let $T_{mm'}^a$ be the matrix elements of its generators. Then we can define a corresponding operator, in second quantized language, as follows:

$$T^a = \sum_{mm'} T_{mm'}^a f_m^\dagger f_{m'}. \quad (4.17)$$

Then, the commutator of an annihilation operator f_m with T^a is given by

$$[f_m, T^a] = \sum_{m', m''} T_{m'm''}^a [f_m, f_{m'}^\dagger f_{m''}] = \sum_{m''} T_{mm''}^a f_{m''}. \quad (4.18)$$

In the case of an infinitesimal $SU(N)$ rotation, the rotation operator has the form

$$U = 1 - i \sum_a T^a \omega_a, \quad (4.19)$$

where ω_a are the infinitesimal angles of rotation. We then have

$$U^\dagger f_m U = f_m - i \sum_a \omega_a [f_m, T^a] = \sum_{m'} U_{mm'} f_{m'}, \quad (4.20)$$

with $U_{mm'} = 1 - i \sum_a T_{mm'}^a \omega_a$, which is the definition an irreducible tensor operator of Eq. (1.21).

From there, we can establish further irreducible tensor operators by coupling the creation and annihilation operator multiplets and decomposing this product. This is done in full analogy to decomposing a product representation, the only difference being that the the carrier space is a space of operators.

Chapter 5

Conclusions and Outlook

Although the original goal of writing a working NRG code which is able to exploit arbitrary $SU(N)$ symmetries has not yet been fully implemented (due to time constraints), we have overcome the major hurdles on the way. A program which can compute any set of $SU(N)$ Clebsch-Gordan coefficients has been developed in the course of this thesis. Meanwhile, our collaborators in Budapest, Gergely Zaránd and Pascu Moca are in the process of extending their NRG code, which has been laid out in a flexible fashion from the beginning, to take into account outer multiplicity labels, which do not occur with $SU(2)$.

The outer multiplicity problem is one of the main differences between $SU(2)$ and general $SU(N)$ and requires fundamental changes in the treatment of symmetry multiplets in the Budapest NRG code. Apart from that, the only jigsaw piece which is missing is the set-up of a suitable model, which involves manually grouping local states of the Wilson chain into symmetry multiplets. However, part of this work has already been broached in Sec. 4.6. Thus, first numerical results can be expected within the next few weeks.

Besides, the development of a code for computing $SU(N)$ Clebsch-Gordan coefficients will hopefully prove useful in other projects, too, as quantum impurity models are not the only models which possess $SU(N)$ symmetries. For example, already in the near vicinity of NRG, namely in the context of DMRG, non-Abelian symmetries stir interest [4]. Eventually, we might release the Clebsch-Gordan coefficient code as a self-contained package.

After the proof of principle will have been accomplished, physical challenges are lingering. Multi-channel Kondo models have already found applications in describing magnetic impurities in simple metals [31], for example. Our collaborator P. Moca has indicated that there exists an application of a $SU(4)$ model to carbon nanotubes.

Additionally, some questions of rather technical nature have arisen in the course of this thesis:

- Research faster algorithms for the computation of Clebsch-Gordan coefficients. This would allow computing them on demand and could lead to significant

memory savings. [32] might provide a good starting point. A distant goal would be to establish algebraic formulas for Clebsch-Gordan coefficients.

- Find a canonical way to resolve the outer multiplicity problem. The attempts we have been able to track down include embedding $SU(N)$ into a larger group, e.g. $U(2N)$, and using further operators in addition to the Casimir operators to distinguish between irreps.
- Further develop the construction of irreducible tensor operators in the context of NRG. It would be convenient to have irreducible tensor operators automatically constructed by a computer.
- Write a massively parallel implementation of NRG. As symmetries cut the Hamiltonian into small blocks which can be diagonalized independently, the run time of a such an implementation should scale well with the number of processors. However, once in each iteration, all processor have to be synchronized.
- Find out if there exists an easier way than Eq. (4.15) to obtain the reduced matrix elements of the hopping terms $H_{k-1,k}$ in NRG. This might be possible by using some completeness relation for the Clebsch-Gordan coefficients. For example, [4] claims to completely have factored out Clebsch-Gordan coefficients of DMRG with non-Abelian symmetries. As DMRG as well as NRG generate matrix product states, this might also be feasible for NRG.
- Formulate non-Abelian symmetries in the language of matrix product states [28]. This a project we will attack in the medium term.

Last, but not least, it would be desirable to have the formulation of $SU(N)$ representation theory presented in this thesis be integrated into the curricula of physics students as a natural extension of quantum angular momentum. Let us hope that exploiting unitary symmetries will become as common as factoring out the angular dependence of the hydrogen atom.

Appendix A

Mapping of irreps and states onto the natural numbers

For numerical codes dealing with Young diagrams, it is useful to identify each Young diagram by a unique number. To this end, we need a one-to-one mapping between the set of all $SU(N)$ Young diagrams (for given N) and the set of nonnegative integers. We shall construct such a mapping by devising an ordering rule for Young diagrams, using this rule to arrange all possible diagrams in a list of increasing order, and labeling each diagram by its position in this list.

Similarly, we would like to map Young tableaux (or equivalently, Gelfand-Tsetlin patterns) to matrix indices, so we also need a one-to-one mapping between the set of all tableaux with the shape of a given diagram and the integers from 1 to the dimension of the irrep labeled by said diagram. Therefore, we also define an order on Gelfand-Tsetlin patterns of a given irrep and proceed analogously.

A.1 Identifying Young diagrams with a single number

For Young diagrams, we choose the following ordering rule (formalized below): the “smaller” of two Young diagrams is taken to be the one with the smaller number of boxes in the topmost row; in case of a tie, strike out rows (one by one, starting from the top down) and recompare, until the tie is broken. Table A.1 shows the first few Young diagrams of $SU(4)$, arranged in increasing order.

We adopt throughout the convention for $SU(N)$ Young diagrams that columns with N boxes will be dropped (Sec. 3.2.1, rule 5), such that each diagram contains at most $N - 1$ rows. Each such diagram can be characterized by sequence of $N - 1$ integers (b_1, \dots, b_{N-1}) satisfying $b_k \geq b_{k+1}$, where $b_k \geq 0$ specifies the number of boxes in row k . Given two Young diagrams, $Y(\{b_k\})$ and $Y'(\{b'_k\})$, we assign the order $Y' < Y$ if and only if, for the smallest index (say l) for which $b'_l \neq b_l$, we have $b'_l < b_l$.

Using this ordering rule, all possible $SU(N)$ Young diagrams can be arranged in a list of increasing order and uniquely labeled by a nonnegative integer, say $M(Y)$, giving its position in this list. To determine $M(Y)$ for a given diagram Y , we simply

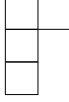
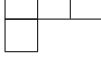
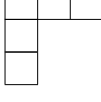
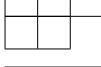
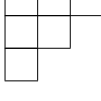
$M(Y)$	Young diagram Y	(b_1, b_2, b_3)
0	(empty)	(0, 0, 0)
1		(1, 0, 0)
2		(1, 1, 0)
3		(1, 1, 1)
4		(2, 0, 0)
5		(2, 1, 0)
6		(2, 1, 1)
7		(2, 2, 0)
8		(2, 2, 1)
9		(2, 2, 2)
10		(3, 0, 0)
11		(3, 1, 0)
12		(3, 1, 1)
13		(3, 2, 0)
14		(3, 2, 1)

Table A.1. The first few Young diagrams of $SU(4)$ (excluding diagrams containing columns of length 4), arranged in increasing order. In the right column, corresponding sequences of row lengths (b_1, b_2, b_3) , where b_k gives the number of boxes in row k , are shown.

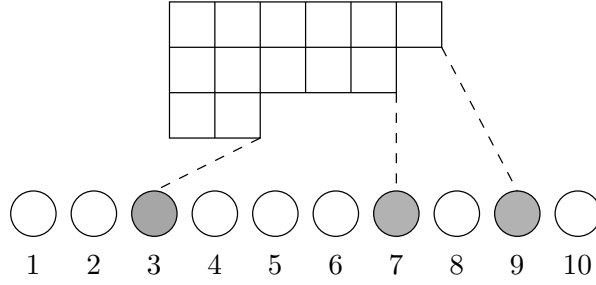


Figure A.1. Example of a item-drawing outcome and the corresponding Young diagram. The shaded circles denote drawn items, which, in turn, determine the “step positions” in the Young diagram. Here, $(d_1, d_2, d_3) = (3, 7, 9)$ and $(b_1, b_2, b_3) = (6, 5, 2)$.

count the number of smaller diagrams Y' : this number is given by the number (say $J_1(Y)$) of all diagrams Y' having less boxes in the first row than Y ($b'_1 < b_1$), plus the number of all Y' s with an equal number of boxes in the first row, but less boxes in the second row ($b'_1 = b_1$ and $b'_2 < b_2$), etc. Thus,

$$M(Y) = \sum_{l=1}^{N-1} J_l(Y), \quad (\text{A.1})$$

where $J_l(Y)$ is the number of diagrams having $b'_k = b_k$ for all $k < l$, and $b'_l < b_l$.

To calculate $J_l(Y)$, we have to consider the combinatorial problem of counting the number of Youngs diagrams with a given number of rows (say r) and with a given maximum number of boxes in the top row (say m). However, this number is the same as the number of ways to draw r items out of a collection of $r + m$ items, and thus is given by $\binom{r+m}{r}$. This analogy can be seen as follows: Let us denote the items by the integers $1, \dots, r + m$ and the drawn items by r integers (d_1, \dots, d_r) , where $d_1 < d_2 < \dots < d_r$. For this specific outcome, we construct a corresponding Young diagram (b_1, \dots, b_{N-1}) by the rule $b_k = d_{r+1-k} - (r + 1 - k)$ (see Fig. A.1).

Thus, we have

$$J_l(Y) = \binom{N - l + b_l - 1}{N - l}, \quad (\text{A.2})$$

and, consequently,

$$M(Y) = \sum_{l=1}^{N-1} \binom{N - l + b_l - 1}{N - l}. \quad (\text{A.3})$$

$$\begin{array}{c}
\begin{pmatrix} 2 & 0 & 0 \\ & 2 & 0 \\ & & 2 \end{pmatrix} < \begin{pmatrix} 2 & 0 & 0 \\ & 2 & 0 \\ & & 1 \end{pmatrix} < \begin{pmatrix} 2 & 0 & 0 \\ & 2 & 0 \\ & & 0 \end{pmatrix} \\
< \begin{pmatrix} 2 & 0 & 0 \\ & 1 & 0 \\ & & 1 \end{pmatrix} < \begin{pmatrix} 2 & 0 & 0 \\ & 1 & 0 \\ & & 0 \end{pmatrix} < \begin{pmatrix} 2 & 0 & 0 \\ & 0 & 0 \\ & & 0 \end{pmatrix}
\end{array}$$

Figure A.2. Example of the ordering of all Gelfand-Tsetlin patterns with top row $(2, 0, 0)$.

A.2 Mapping of Gelfand-Tsetlin patterns to matrix indices

In analogy to the ordering we have defined on Young diagrams, we introduce an ordering on the set of Gelfand-Tsetlin patterns of a given irrep (i.e. given top row of the pattern). Let $G(\{m_{k,l}\})$ and $G'(\{m'_{k,l}\})$ (where $1 \leq k \leq l \leq N$) denote two patterns with $m_{k,N} = m'_{k,N}$ for $k = 1, \dots, N$. Furthermore, let (p, q) denote the “largest” index for which $m_{p,q} \neq m'_{p,q}$, i.e. $m_{k,l} = m'_{k,l}$ for $l > q$ and for $l = q$ but $k < p$. We then define $G' < G$ if and only if $m'_{p,q} > m_{p,q}$. An example of this ordering is given in Fig. A.2.

We map each Gelfand-Tsetlin pattern G to a nonnegative integer $H(G)$ by counting the number of smaller Gelfand-Tsetlin patterns, i.e.

$$H(G) = \#\{G' | G' < G\} + 1. \quad (\text{A.4})$$

This number can be determined by generating the pattern (say $\tilde{G}(\{\tilde{m}_{k,l}\})$) located directly in front of G in the list of all patterns in increasing order, the pattern preceding \tilde{G} , and so on, until we arrive at the head of this list. To construct the predecessor of the pattern G , we start by finding the “smallest” index (r, s) such that $m_{r,s}$ can be increased without violating the betweenness condition (see Eq. (3.16)), i.e. $m_{k,l} = m_{k,l+1}$ for $l < s$ and for $l = s$ but $k > r$. We then set

$$\tilde{m}_{k,l} = \begin{cases} m_{k,l} & \text{for } l > s \text{ and for } l = s \text{ but } k < r \\ 1 + m_{k,l} & \text{for } (k, l) = (r, s) \\ m_{k+1, l+1} & \text{for } l < s \text{ and for } l = s \text{ but } k > r. \end{cases} \quad (\text{A.5})$$

The number $H(G)$ is, of course, the number of times we can repeat the process of constructing a preceding pattern.

Appendix B

Derivation of Eq. (4.15)

We start from the reduced matrix element and expand it in terms of ordinary matrix elements (Eq. (1.26)). As $H_{k-1,k}$ is a scalar operator, this reduced matrix element does not carry an outer multiplicity label, and the Clebsch-Gordan coefficient in Eq. (1.26) immediately reduces to Kronecker deltas. So, we obtain

$$\begin{aligned} & \langle n'_{k-1}, j'_{k-1}, \tilde{n}'_k, \tilde{j}'_k, j', \alpha' | H_{k-1,k} | n_{k-1}, j_{k-1}, \tilde{n}_k, \tilde{j}_k, j, \alpha \rangle \\ &= \sum_{m'} \frac{\delta_{j',j}}{\dim j} \langle n'_{k-1}, j'_{k-1}, \tilde{n}'_k, \tilde{j}'_k, j', m', \alpha' | H_{k-1,k} | n_{k-1}, j_{k-1}, \tilde{n}_k, \tilde{j}_k, j, m', \alpha \rangle. \end{aligned} \quad (\text{B.1})$$

Then, we expand the bra and the ket which sandwich $H_{k-1,k}$ in terms of the coupled basis states (i.e. tensor products of block and local states). This is done by applying Eq. (4.11) twice:

$$\begin{aligned} & \sum_{m'} \frac{\delta_{j',j}}{\dim j} \langle n'_{k-1}, j'_{k-1}, \tilde{n}'_k, \tilde{j}'_k, j', m', \alpha' | H_{k-1,k} | n_{k-1}, j_{k-1}, \tilde{n}_k, \tilde{j}_k, j, m', \alpha \rangle \\ &= \sum_{m'} \sum_{m'_{k-1}} \sum_{\tilde{m}'_k} \sum_{m_{k-1}} \sum_{\tilde{m}_k} \frac{\delta_{j',j}}{\dim j} \\ & \quad \langle j', m', \alpha' | j'_{k-1}, m'_{k-1}; \tilde{j}'_k, \tilde{m}'_k \rangle \langle j_{k-1}, m_{k-1}; \tilde{j}_k, \tilde{m}_k | j, m', \alpha \rangle \\ & \quad \langle n'_{k-1}, j'_{k-1}, m'_{k-1}; \tilde{n}'_k, \tilde{j}'_k, \tilde{m}'_k | H_{k-1,k} | n_{k-1}, j_{k-1}, m_{k-1}; \tilde{n}_k, \tilde{j}_k, \tilde{m}_k \rangle. \end{aligned} \quad (\text{B.2})$$

At this point, we insert Eq. (4.14) for $H_{k-1,k}$ and pull apart the coupled basis states, as $f_{k-1,m}^\dagger$ and $f_{k-1,m}$ act only on block states, and $f_{k,m}^\dagger$ and $f_{k,m}$ act only on local states. Moreover, we take the complex conjugate of the matrix elements of the creation operators so that only annihilation operators remain:

$$\begin{aligned} & \sum_{m'} \sum_{m'_{k-1}} \sum_{\tilde{m}'_k} \sum_{m_{k-1}} \sum_{\tilde{m}_k} \frac{\delta_{j',j}}{\dim j} \\ & \quad \langle j', m', \alpha' | j'_{k-1}, m'_{k-1}; \tilde{j}'_k, \tilde{m}'_k \rangle \langle j_{k-1}, m_{k-1}; \tilde{j}_k, \tilde{m}_k | j, m', \alpha \rangle \\ & \quad \langle n'_{k-1}, j'_{k-1}, m'_{k-1}; \tilde{n}'_k, \tilde{j}'_k, \tilde{m}'_k | H_{k-1,k} | n_{k-1}, j_{k-1}, m_{k-1}; \tilde{n}_k, \tilde{j}_k, \tilde{m}_k \rangle \end{aligned}$$

$$\begin{aligned}
&= \sum_{m'} \sum_{m'_{k-1}} \sum_{\tilde{m}'_k} \sum_{m_{k-1}} \sum_{\tilde{m}_k} \sum_m \frac{\delta_{j',j}}{\dim j} \\
&\quad \langle j', m', \alpha' | j'_{k-1}, m'_{k-1}; \tilde{j}'_k, \tilde{m}'_k \rangle \langle j_{k-1}, m_{k-1}; \tilde{j}_k, \tilde{m}_k | j, m', \alpha \rangle \\
&\quad \left(\langle n_{k-1}, j_{k-1}, m_{k-1} | f_{k-1,m} | n'_{k-1}, j'_{k-1}, m'_{k-1} \rangle^* \langle \tilde{n}'_k, \tilde{j}'_k, \tilde{m}'_k | f_{k,m} | \tilde{n}_k, \tilde{j}_k, \tilde{m}_k \rangle \right. \\
&\quad \left. + \langle n'_{k-1}, j'_{k-1}, m'_{k-1} | f_{k-1,m} | n_{k-1}, j_{k-1}, m_{k-1} \rangle \langle \tilde{n}_k, \tilde{j}_k, \tilde{m}_k | f_{k,m} | \tilde{n}'_k, \tilde{j}'_k, \tilde{m}'_k \rangle^* \right). \tag{B.3}
\end{aligned}$$

What remains is to express the ordinary matrix elements in terms of reduced matrix elements by virtue of Eq. (1.25):

$$\begin{aligned}
&\sum_{m'} \sum_{m'_{k-1}} \sum_{\tilde{m}'_k} \sum_{m_{k-1}} \sum_{\tilde{m}_k} \sum_m \frac{\delta_{j',j}}{\dim j} \\
&\quad \langle j', m', \alpha' | j'_{k-1}, m'_{k-1}; \tilde{j}'_k, \tilde{m}'_k \rangle \langle j_{k-1}, m_{k-1}; \tilde{j}_k, \tilde{m}_k | j, m', \alpha \rangle \\
&\quad \left(\langle n_{k-1}, j_{k-1}, m_{k-1} | f_{k-1,m} | n'_{k-1}, j'_{k-1}, m'_{k-1} \rangle^* \langle \tilde{n}'_k, \tilde{j}'_k, \tilde{m}'_k | f_{k,m} | \tilde{n}_k, \tilde{j}_k, \tilde{m}_k \rangle \right. \\
&\quad \left. + \langle n'_{k-1}, j'_{k-1}, m'_{k-1} | f_{k-1,m} | n_{k-1}, j_{k-1}, m_{k-1} \rangle \langle \tilde{n}_k, \tilde{j}_k, \tilde{m}_k | f_{k,m} | \tilde{n}'_k, \tilde{j}'_k, \tilde{m}'_k \rangle^* \right) \\
&= \sum_{m'} \sum_{m'_{k-1}} \sum_{\tilde{m}'_k} \sum_{m_{k-1}} \sum_{\tilde{m}_k} \sum_m \sum_{\alpha_{k-1}} \sum_{\tilde{\alpha}_k} \frac{\delta_{j',j}}{\dim j} \\
&\quad \langle j', m', \alpha' | j'_{k-1}, m'_{k-1}; \tilde{j}'_k, \tilde{m}'_k \rangle \langle j_{k-1}, m_{k-1}; \tilde{j}_k, \tilde{m}_k | j, m', \alpha \rangle \\
&\quad \left(\langle j_{k-1}, m_{k-1}, \alpha_{k-1} | j_f, m; j'_{k-1}, m'_{k-1} \rangle^* \langle \tilde{j}'_k, \tilde{m}'_k, \tilde{\alpha}_k | j_f, m; \tilde{j}_k, \tilde{m}_k \rangle \right. \\
&\quad \langle n_{k-1}, j_{k-1} || f_{k-1} || n'_{k-1}, j'_{k-1} \rangle^* \langle \tilde{n}'_k, \tilde{j}'_k || f_k || \tilde{n}_k, \tilde{j}_k \rangle \\
&\quad + \langle j'_{k-1}, m'_{k-1}, \alpha_{k-1} | j_f, m; j_{k-1}, m_{k-1} \rangle \langle \tilde{j}_k, \tilde{m}_k, \tilde{\alpha}_k | j_f, m; \tilde{j}'_k, \tilde{m}'_k \rangle^* \\
&\quad \left. \langle n'_{k-1}, j'_{k-1} || f_{k-1} || n_{k-1}, j_{k-1} \rangle \langle \tilde{n}_k, \tilde{j}_k || f_k || \tilde{n}'_k, \tilde{j}'_k \rangle^* \right). \tag{B.4}
\end{aligned}$$

Here, j_f is the representation label of the irreducible tensor operators f_{k-1} and f_k , which have components $f_{k-1,m}$ and $f_{k,m}$, respectively. Now, we are done; the right-hand side depends only on reduced matrix elements of f_{k-1} and f_k and some Clebsch-Gordan coefficients, which all are known quantities.

Appendix C

Program code for computing $SU(N)$ Clebsch-Gordan coefficients

The following source code is a MATLAB implementation of the ideas presented in Ch. 3.

C.1 Enumerating irreps

The following function returns the index of an irrep, as App. A.1. For example `irrep_index([3 1 0])` returns “7”.

```
1 function result = irrep_index(irrep)
    result = 0;
    aux_sum = 0;
    for k = 1:length(irrep) - 1
        aux_sum = aux_sum + irrep(k) - irrep(k + 1);
6         if aux_sum > 0
            result = result + nchoosek(k + aux_sum - 1, k);
        end
    end
end
```

C.2 Mapping Gelfand-Tsetlin patterns to matrix indices

The following function returns the matrix index of a Gelfand-Tsetlin pattern. Takes as a call parameter a two-dimensional array $a(k, l)$, which corresponds to the entry m_{kl} of the pattern. For example, `pattern_index([[0 0 2]; [0 0 0]; [0 0 0]])` returns 6 because this is the sixth pattern in Fig. (A.2).

```
function result = pattern_index(pattern)
    result = 1;

    n = size(pattern, 1);
5     while true
        col = 1;
```

```

row = 1;
while row < n && pattern(col, row) == pattern(col, row + 1)
  col = col - 1;
  if col == 0
    row = row + 1;
    col = row;
  end
end
end

if row >= n
  break
end

pattern(col, row) = pattern(col, row) + 1;

while true
  col = col + 1;
  if col > row
    row = row - 1;
    col = 1;
  end
  if row == 0
    break
  end
  pattern(col, row) = pattern(col + 1, row + 1);
end

result = result + 1;
end
end

```

C.3 Dimension of an irrep

Returns the dimension of an irrep. For example, the call `irrep_dimension([3 1 0])` returns “15”, the dimension of the $SU(3)$ irrep $\begin{smallmatrix} \square & \square \\ \square & \end{smallmatrix}$. Straightforward implementation of Eq. (3.17).

```

function result = irrep_dimension(irrep)
  result = 1;
  for k = 2:length(irrep)
    for l = 1:k - 1
      result = result * ((irrep(l) - 1) - (irrep(k) - k)) / (k - 1);
    end
  end
  result = int32(result);
end

```

C.4 Matrix element of lowering operator

A one-to-one implementation of Eq. (3.18). Called internally by `lowering_operator`.

```

1  function result = lowering_op_matrix_element(pattern, col, row)
    result = 1;

    row = row + 1;
    for k = 1:row
6     result = result * ((pattern(k, row) - k) ...
                        - (pattern(col, row - 1) - col) + 1);
    end

    for k = 1:row - 2
11    result = result * ((pattern(k, row - 2) - k) ...
                        - (pattern(col, row - 1) - col));
    end

    for k = 1:row - 1
16    if k == col
        continue
    end
    result = result / (((pattern(k, row - 1) - k) ...
                       - (pattern(col, row - 1) - col) + 1) ...
                       * ((pattern(k, row - 1) - k) ...
                          - (pattern(col, row - 1) - col)));
21
    end

    result = sqrt(-result);
26 end

```

C.5 Construction of the lowering operator matrix

Returns the matrix representation of a lowering operator. For example, `lowering_operator([2 1 0], 2)` returns the matrix representation of $J_-^{(2)}$ in the SU(3) irrep $\begin{smallmatrix} \square & \square \\ & \square \end{smallmatrix}$.

```

function result = lowering_operator(irrep, operator_index)
    n = length(irrep);
    working_pattern = zeros(n);
4    working_pattern(:, n) = reshape(irrep, 1, n);
    dimension = irrep_dimension(irrep);
    result = zeros(dimension);

    function generate_all_patterns(col, row)
9        if col > row
            col = 1;
            row = row - 1;
        end

```

```

14     if row == 0
        result_col = pattern_index(working_pattern);
        for k = 1:operator_index
            if working_pattern(k, operator_index) - 1 ...
19                >= working_pattern(k + 1, operator_index + 1) ...
                && (k == operator_index ...
                || working_pattern(k, operator_index) - 1 ...
                >= working_pattern(k, operator_index - 1))
                working_pattern(k, operator_index) = ...
24                working_pattern(k, operator_index) - 1;
                result_row = pattern_index(working_pattern);
                working_pattern(k, operator_index) = ...
                working_pattern(k, operator_index) + 1;
                result(result_row, result_col) = ...
29                lowering_op_matrix_element(working_pattern, ...
                k, operator_index);
            end
        end
        return
    end
34     for k = working_pattern(col+1, row+1):working_pattern(col, row+1)
        working_pattern(col, row) = k;
        generate_all_patterns(col + 1, row);
    end
39     end
    generate_all_patterns(1, n - 1);
end

```

C.6 Weight vector

Returns the weight of a state. Parameters are the set of lowering operators, and the index of the desired state. Called internally by `clebsch_matrix`.

```

function result = weight_vector(lowering_operators, index)
    dimension = size(lowering_operators, 1);
3   n = 1 + size(lowering_operators, 2) / dimension;
    result = zeros(1, n - 1);

    for k = 1:n - 1
        result(k) = sum(lowering_operators(:, ...
8                dimension * (k - 1) + index).^2) ...
                - sum(lowering_operators(index, ...
                dimension * (k - 1) + 1:dimension * k).^2);
    end
end

```

C.7 Clebsch-Gordan coefficients of the highest-weight state

Returns the Clebsch-gordan coefficients of a highest-weight state with a given weight. Implementation of the linear system of Eq. (3.24). Called internally by `clebsch_matrix`.

```

function result = highest_weight_states(lowering_operators, given_weight)
    dimension = size(lowering_operators, 1);
3     n = size(lowering_operators, 2) / dimension;
    is_good = true(dimension, 1);

    for k = 1:dimension
        if norm(weight_vector(lowering_operators, k) - given_weight) > 1e-3
8             is_good(k) = false;
        end
    end

    identity = eye(dimension);
13    result = identity(:, is_good) ...
        * null(lowering_operators' * identity(:, is_good));
end

```

C.8 Decomposition of a product representation

Returns the product representation decomposition, as in Sec. 3.2.4. Call as `decompose_product([2 1 0], [2 1 0])` to obtain the result of Eq. (3.14).

```

function result = decompose_product(irrep1, irrep2);
    n = length(irrep1);
    nr_of_direct_summands = 0;
    result = zeros(n, min(irrep_dimension(irrep1), irrep_dimension(irrep2)));
5

    working_pattern = zeros(n);
    working_pattern(:, n) = reshape(irrep1, n, 1);
    resulting_pattern = reshape(irrep2, n, 1);

10    function fill_working_pattern(col, row)
        if col > n
            nr_of_direct_summands = nr_of_direct_summands + 1;
            result(:, nr_of_direct_summands) = resulting_pattern;
            return
15        end

        if col > row
            resulting_pattern(col) = resulting_pattern(col) ...
                + working_pattern(col, col);
20        fill_working_pattern(col + 1, n - 1);
            resulting_pattern(col) = resulting_pattern(col) ...
                - working_pattern(col, col);

        return;
    end

```

```

25     lower_limit = max(0, working_pattern(col, row + 1) ...
                        - resulting_pattern(row) ...
                        + resulting_pattern(row + 1));
30     if row == n - 1
        lower_limit = max(lower_limit, working_pattern(col + 1, row + 1));
    end

    upper_limit = working_pattern(col, row + 1);
    if col > 1
35         upper_limit = min(upper_limit, working_pattern(col - 1, row - 1));
    end
    if row > 1 && col == row
        upper_limit = min(upper_limit, resulting_pattern(row - 1) ...
                        - resulting_pattern(row));
40     end

    for k = lower_limit:upper_limit
        working_pattern(col, row) = k;
        resulting_pattern(row + 1) = resulting_pattern(row + 1) ...
            + (working_pattern(col, row + 1) - k);
45         fill_working_pattern(col, row - 1);
        resulting_pattern(row + 1) = resulting_pattern(row + 1) ...
            - (working_pattern(col, row + 1) - k);
    end
50 end

fill_working_pattern(1, n - 1);
result = result(:, 1:nr_of_direct_summands);
end

```

C.9 Calculation of the matrix of Clebsch-Gordan coefficients

Return the full matrix of Clebsch-Gordan coefficients. For example, `clebsch_matrix([1 0], [1 0])` return the Clebsch-Gordan coefficients of the coupling of two one-half spins.

```

1  function result = clebsch_matrix(irrep1, irrep2)
    dimension1 = irrep_dimension(irrep1);
    dimension2 = irrep_dimension(irrep2);
    disp(sprintf('Coupled representation has dim %d * %d = %d.', ...
6         dimension1, dimension2, dimension1 * dimension2));

    result = zeros(dimension1 * dimension2);
    n = length(irrep1);

    old_lowering_operators = cell(n - 1, 1);
11    for k = 1:n - 1
        old_lowering_operators{k} = kron(lowering_operator(irrep1, k), ...
            eye(dimension2)) ...
            + kron(eye(dimension1), ...

```

```

16         lowering_operator(irrep2, k));
end
dimension_sum = 0;
new_lowering_operators = cell(n - 1, 1);
21 for direct_summand = unique(decompose_product(irrep1, irrep2)', 'rows')
    this_dimension = irrep_dimension(direct_summand);
    for k = 1:n - 1
        new_lowering_operators{k} = lowering_operator(direct_summand, k);
    end
26 for w = highest_weight_states([old_lowering_operators{:}], ...
    weight_vector([new_lowering_operators{:}], 1))
    disp(sprintf('Found irrep with dim %d.', this_dimension));
31 old_states = zeros(dimension1 * dimension2, this_dimension);
old_states(:, 1) = w;
new_states = zeros(this_dimension);
new_states(1, 1) = 1;
36 done_states = int32(0);
have_states = int32(1);
while have_states < this_dimension
    done_states = done_states + 1;
    for k = 1:n - 1
41 new_states(:, have_states + 1) = ...
        new_lowering_operators{k} * ...
        new_states(:, done_states);
        new_norm = norm(new_states(:, have_states + 1));
46 if new_norm > 1e-4 && rank(new_states) > have_states
            have_states = have_states + 1;
            new_states(:, have_states) = ...
                new_states(:, have_states) ./ new_norm;
            old_states(:, have_states) = ...
51 old_lowering_operators{k} * ...
                * old_states(:, done_states);
            old_norm = norm(old_states(:, have_states));
            old_states(:, have_states) = ...
                old_states(:, have_states) ./ old_norm;
56 end
        if have_states >= this_dimension
            break
        end
    end
61 end
    result(:, dimension_sum + 1:dimension_sum + this_dimension) = ...
        (new_states' \ old_states');
66 dimension_sum = dimension_sum + this_dimension;
end
end
end
end

```


Bibliography

- [1] A. Weichselbaum and J. von Delft, “Sum-Rule conserving spectral functions from the numerical renormalization group,” *Physical Review Letters*, vol. 99, no. 7, pp. 076402–4, 2007.
- [2] H. R. Krishna-murthy, J. W. Wilkins, and K. G. Wilson, “Renormalization-group approach to the anderson model of dilute magnetic alloys. i. static properties for the symmetric case,” *Physical Review B*, vol. 21, p. 1003, Feb. 1980. Copyright (C) 2009 The American Physical Society; Please report any problems to prola@aps.org.
- [3] A. I. Tóth, C. P. Moca, O. Legeza, and G. Zaránd, “Density matrix numerical renormalization group for non-abelian symmetries,” *Physical Review B (Condensed Matter and Materials Physics)*, vol. 78, no. 24, p. 245109, 2008.
- [4] I. P. McCulloch and M. Gulácsi, “The non-Abelian density matrix renormalization group algorithm,” *Europhysics Letters*, vol. 57, no. 6, p. 852, 2002.
- [5] J. D. Louck, “Recent progress toward a theory of tensor operators in the unitary groups,” *American Journal of Physics*, vol. 38, no. 1, pp. 3–42, 1970.
- [6] J. F. Cornwell, *Group Theory in Physics*, vol. I of *Techniques in Physics 7*. London: Academic Press, 1984.
- [7] J. F. Cornwell, *Group Theory in Physics*, vol. II of *Techniques in Physics 7*. London: Academic Press, 1984.
- [8] J. J. Sakurai, *Modern quantum mechanics*. Reading, MA: Addison-Wesley, revised ed., 1994.
- [9] A. R. Edmonds, *Angular momentum in quantum mechanics*, vol. 4 of *Investigations in physics*. Princeton, N.J.: Princeton Univ. Press, 1957.
- [10] M. E. Rose, *Elementary theory of angular momentum*. Structure of matter series, New York: Wiley, 1957.
- [11] A. Weichselbaum, “Su(2) clebsches via diagonalization of casimir operators.” Private communication, September 2009.

-
- [12] W. Fulton and J. Harris, *Representation theory: a first course*, vol. 129 of *Graduate texts in mathematics*. New York: Springer, 9 ed., 2004.
- [13] J. E. Humphreys, *Introduction to Lie algebras and representation theory*, vol. 9 of *Graduate texts in mathematics*. New York: Springer, 1972.
- [14] R. N. Cahn, *Semi-simple Lie Algebras and their representations*, vol. 59 of *Frontiers in physics*. Menlo Park, Calif.: Benjamin/Cummings, 1984.
- [15] H. Boerner, *Darstellungen von Gruppen: mit Berücksichtigung der Bedürfnisse der modernen Physik*, vol. 74 of *Die Grundlehren der mathematischen Wissenschaften in Einzeldarstellungen*. Berlin: Springer, 2., überarb. Aufl. ed., 1967.
- [16] M. Hamermesh, *Group theory and its applications to physical problems*. Addison-Wesley series in physics, Reading, Mass. : Addison-Wesley: Addison-Wesley, 2. print ed., 1964.
- [17] D. B. Lichtenberg, *Unitary symmetry and elementary particles*. New York: Acad.Pr., 1978.
- [18] A. O. Barut and R. Raczyk, *Theory of group representations and applications*. Warszawa: PWN-Polish Scientific Publ., 2nd, revised ed., 1986.
- [19] J. D. Louck, *Unitary Symmetry And Combinatorics*. World Scientific Publishing Company, Sept. 2008.
- [20] M. A. A. van Leeuwen, “The littlewood-richardson rule, and related combinatorics,” *math.CO/9908099*, 2007.
- [21] J. B. Remmel and R. Whitney, “Multiplying schur functions,” *J. Algorithms*, vol. 5, no. 4, pp. 471–487, 1984.
- [22] G. Zaránd, “A method for resolving the outer multiplicity problems.” Private communication, July 2009.
- [23] K. G. Wilson, “The renormalization group: Critical phenomena and the kondo problem,” *Reviews of Modern Physics*, vol. 47, p. 773, Oct. 1975. Copyright (C) 2009 The American Physical Society; Please report any problems to prola@aps.org.
- [24] K. G. Wilson, “The renormalization group and critical phenomena,” *Rev. Mod. Phys.*, vol. 55, pp. 583–600, Jul 1983.

-
- [25] H. R. Krishna-murthy, J. W. Wilkins, and K. G. Wilson, “Renormalization-group approach to the anderson model of dilute magnetic alloys. II. static properties for the asymmetric case,” *Physical Review B*, vol. 21, p. 1044, Feb. 1980. Copyright (C) 2009 The American Physical Society; Please report any problems to prola@aps.org.
- [26] R. Bulla, T. A. Costi, and T. Pruschke, “Numerical renormalization group method for quantum impurity systems,” *Reviews of Modern Physics*, vol. 80, pp. 395–56, Apr. 2008.
- [27] R. Peters, T. Pruschke, and F. B. Anders, “Numerical renormalization group approach to green’s functions for quantum impurity models,” *Physical Review B (Condensed Matter and Materials Physics)*, vol. 74, pp. 245114–12, Dec. 2006.
- [28] A. Weichselbaum, F. Verstraete, U. Schollwöck, J. I. Cirac, and J. von Delft, “Variational matrix product state approach to quantum impurity models,” *cond-mat/0504305*, Apr. 2005.
- [29] F. B. Anders and A. Schiller, “Spin precession and real-time dynamics in the kondo model: Time-dependent numerical renormalization-group study,” *Physical Review B (Condensed Matter and Materials Physics)*, vol. 74, no. 24, p. 245113, 2006.
- [30] J. von Delft, “Irreducible tensor operators in nrg.” Private communication, September 2009.
- [31] P. Schlottmann and P. D. Sacramento, “Multichannel kondo problem and some applications,” *Advances in Physics*, vol. 42, no. 6, pp. 641–682, 1993.
- [32] S. Gliske, W. Klink, and T. Ton-That, “Algorithms for computing $U(N)$ clebsch gordan coefficients,” *Acta Applicandae Mathematicae: An International Survey Journal on Applying Mathematics and Mathematical Applications*, vol. 95, no. 1, pp. 51–72, 2007.
- [33] S. Alisauskas and Y. F. Smirnov, “Multiplicity-free $uq(n)$ coupling coefficients,” *Journal of Physics A: Mathematical and General*, vol. 27, no. 17, pp. 5925–5939, 1994.
- [34] G. E. Baird and L. C. Biedenharn, “On the representations of the semisimple lie groups. iii. the explicit conjugation operation for $su[\text{sub } n]$,” *Journal of Mathematical Physics*, vol. 5, no. 12, pp. 1723–1730, 1964.

-
- [35] G. E. Baird and L. C. Biedenharn, “On the representations of the semisimple lie groups. ii,” *Journal of Mathematical Physics*, vol. 4, no. 12, pp. 1449–1466, 1963.
- [36] L. C. Biedenharn and D. E. Flath, “On the structure of tensor operators in SU3,” *Communications in Mathematical Physics*, vol. 93, pp. 143–169, June 1984.
- [37] L. C. Biedenharn, A. Giovannini, and J. D. Louck, “Canonical definition of wigner coefficients in u_n ,” *Journal of Mathematical Physics*, vol. 8, pp. 691–700, Apr. 1967.
- [38] L. C. Biedenharn and J. D. Louck, *Angular momentum in quantum physics: theory and application*, vol. 8 of *Encyclopedia of mathematics and its applications*. Reading, Mass: Addison-Wesley, 1981.
- [39] L. C. Biedenharn and J. D. Louck, *The Racah-Wigner algebra in quantum theory*, vol. 9 of *Encyclopedia of mathematics and its applications*. Reading, Mass.: Addison-Wesley, 1981.
- [40] L. C. Biedenharn and J. D. Louck, “A pattern calculus for tensor operators in the unitary groups,” *Communications in Mathematical Physics*, vol. 8, pp. 89–131, June 1968.
- [41] R. L. Blanc and L. C. Biedenharn, “Implementation of the $u(n)$ tensor operator calculus in a vector bargmann hilbert space,” *Journal of Physics A: Mathematical and General*, vol. 22, no. 1, pp. 31–48, 1989.
- [42] R. L. Blanc and D. J. Rowe, “A resolution of the SU(3) outer multiplicity problem and computation of wigner coefficients for SU(3),” *Journal of Physics A: Mathematical and General*, vol. 19, no. 15, pp. 2913–2933, 1986.
- [43] N. Bourbaki, *Algèbres de Lie*. Actualités scientifiques et industrielles, Paris: Hermann, nouv. tirage ed., 1971.
- [44] T. Bröcker and T. t. Dieck, *Representations of compact Lie groups*, vol. 98 of *Graduate Texts in mathematics*. New York: Springer, 1985.
- [45] R. W. Carter, G. Segal, and I. G. Macdonald, *Lectures on Lie groups and Lie algebras*, vol. 32 of *London Mathematical Society student texts*. Cambridge: Cambridge Univ. Press, 4. print ed., 2004.
- [46] S. Chaturvedi and N. Mukunda, “The schwinger $su(3)$ construction - i: Multiplicity problem and relation to induced representations,” *J.Math.Phys.*, vol. 43, pp. 5262–5277, 2002.

-
- [47] J. Chen, P. Wang, Z. Lü, and X. Wu, *Tables of the Clebsch-Gordan, Racah, and subduction coefficients of $SU(n)$ groups*. World Scientific, 1987.
- [48] C. W. Curtis and I. Reiner, *Representation theory of finite groups and associative algebras*, vol. 11 of *Pure and applied mathematics*. New York: Wiley, 1962.
- [49] E. D’Hoker, “Decomposition of representations into basis representations for the classical groups,” *Journal of Mathematical Physics*, vol. 25, no. 1, pp. 1–12, 1984.
- [50] R. Dirl, “Clebsch–Gordan coefficients: General theory,” *Journal of Mathematical Physics*, vol. 20, pp. 659–663, Apr. 1979.
- [51] L. Dornhoff, *Group representation theory: (in two parts)*, vol. . of *Pure and applied mathematics*. New York, NY: Dekker, 1971.
- [52] M. J. Englefield and R. C. King, “Symmetric power sum expansions of the eigenvalues of generalised casimir operators of semi-simple lie groups,” *Journal of Physics A: Mathematical and General*, vol. 13, no. 7, pp. 2297–2317, 1980.
- [53] H. Freudenthal and H. d. Vries, *Linear lie groups*, vol. 35 of *Pure and applied mathematics*. New York, NY: Acad. Press, 1969.
- [54] W. Fulton, *Young tableaux: with applications to representation theory and geometry*, vol. 35 of *London Mathematical Society student texts*. Cambridge: Cambridge Univ. Press, reprinted with corrections ed., 1999.
- [55] D. H. Galvan, S. K. Saha, and W. C. Henneberger, “A simple algorithm for Clebsch–Gordan coefficients,” *American Journal of Physics*, vol. 51, p. 953, Oct. 1983.
- [56] I. M. Gel’fand and M. A. Naimark, *Unitäre Darstellungen der klassischen Gruppen*. (Mathematische Lehrbücher u. Monographien, Berlin: Akademie Verlag, 1957.
- [57] D. M. Gitman and A. L. Shelepin, “Coherent states of the $su(n)$ groups,” *J.Phys. A*, vol. 26, pp. 313–328, 1993.
- [58] S. Gliske, W. H. Klink, and T. Ton-That, “Algorithms for computing generalized $U(N)$ racah coefficients,” *Acta Applicandae Mathematicae: An International Survey Journal on Applying Mathematics and Mathematical Applications*, vol. 88, no. 2, pp. 229–249, 2005.
- [59] W. Greiner and B. Müller, *Quantenmechanik: Symmetrien*. Theoretische Physik, Frankfurt am Main: Deutsch, 4., überarb. und erw. Aufl. ed., 2005.

- [60] V. A. Groza, I. I. Kachurik, and A. U. Klimyk, “On Clebsch–Gordan coefficients and matrix elements of representations of the quantum algebra $u[\text{sub } q](\text{su}[\text{sub } 2])$,” *Journal of Mathematical Physics*, vol. 31, pp. 2769–2780, Dec. 1990.
- [61] B. Gruber, “Relations between “Inner” and “Outer” multiplicities for the classical groups,” *Ann. Inst. Henri Poincaré*, vol. VIII, pp. 43–51, 1968.
- [62] I. I. Guseinov, A. zmen, . Atav, and H. Yksel, “Computation of Clebsch-Gordan and gaunt coefficients using binomial coefficients,” *J. Comput. Phys.*, vol. 122, no. 2, pp. 343–347, 1995.
- [63] N. Jacobson, *Lie algebras*, vol. 10 of *Interscience tracts in pure and applied mathematics*. New York: Interscience Publ., 1962.
- [64] A. A. Kirillov, *Elements of the theory of representations*. Die Grundlehren der mathematischen Wissenschaften ; 220, Berlin [u.a.]: Springer, 1976.
- [65] A. U. Klimyk and A. M. Gavrilik, “Representation matrix elements and Clebsch–Gordan coefficients of the semisimple lie groups,” *Journal of Mathematical Physics*, vol. 20, no. 8, pp. 1624–1642, 1979.
- [66] W. H. Klink and T. Ton-That, “Representations of $sn^*u(n)$ in repeated tensor products of the unitary groups,” *Journal of Physics A: Mathematical and General*, vol. 23, no. 13, pp. 2751–2763, 1990.
- [67] W. H. Klink and T. Ton-That, “Calculation of Clebsch-Gordan and racah coefficients using symbolic manipulation programs,” *J. Comput. Phys.*, vol. 80, no. 2, pp. 453–471, 1989.
- [68] D. E. Knuth, *Sorting and searching*, vol. Vol. 3 of *Addison-Wesley series in computer science and information processing*. Reading, Mass.: Addison-Wesley, 2. printing ed., 1975.
- [69] D. E. Littlewood, *The theory of group characters and matrix representations of groups*. Oxford: Clarendon Press, 2. ed ed., 1950.
- [70] G. W. Mackey, *Unitary group representations in physics, probability, and number theory*, vol. 55 of *Mathematics lecture note series*. Reading, Mass.: The Benjamin/Cummings Publ., 1978.
- [71] I. P. McCulloch, “From density-matrix renormalization group to matrix product states,” *J.STAT.MECH.*, p. P10014, 2007.
- [72] F. D. Murnaghan, *The theory of group representations*. Dover books on advanced mathematics, New York: Dover, 1963.

-
- [73] F. D. Murnaghan, *The unitary and rotation groups*, vol. 3 of *Lectures on applied mathematics*. Washington, D.C.: Spartan Books, 1962.
- [74] J. Nachamkin, “Direct use of young tableau algebra to generate the Clebsch–Gordan coefficients of $SU(2)$,” *Journal of Mathematical Physics*, vol. 16, pp. 2391–2394, Dec. 1975.
- [75] M. A. Naimark and A. I. Stern, *Theory of group representations*, vol. 246 of *Die Grundlehren der mathematischen Wissenschaften*. New York, NY: Springer, 1982.
- [76] P. O’Hara, “Clebsch-gordan coefficients and the binomial distribution,” *quant-ph/0112096*, 2007.
- [77] F. Pan and J. P. Draayer, “A complementary group technique for a resolution of the outer multiplicity problem of $su(n)$: (i) littlewood rule and a complementary group of $su(n)$,” *J.Math.Phys.*, vol. 39, pp. 5631–5641, 1998.
- [78] Y. Saint-Aubin and L. Vinet, *Algebraic methods in physics*. New York: Springer, 2001.
- [79] D. J. Rowe and J. Repka, “An algebraic algorithm for calculating Clebsch–Gordan coefficients; application to $SU(2)$ and $SU(3)$,” *Journal of Mathematical Physics*, vol. 38, no. 8, pp. 4363–4388, 1997.
- [80] K. Schertler and M. H. Thoma, “Combinatorial computation of clebsch-gordan coefficients,” *Annalen Phys.*, vol. 5, p. 103, 1996.
- [81] U. Schollwöck, “The density-matrix renormalization group,” *Rev. Mod. Phys.*, vol. 77, pp. 259–315, Apr 2005.
- [82] J.-P. Serre and G. A. Jones, *Complex semisimple Lie algebras*. Springer monographs in mathematics, Berlin: Springer, reprint of the 1987 ed ed., 2001.
- [83] M. Tinkham, *Group theory and quantum mechanics*. International series in pure and applied physics, New York, N.Y.: McGraw-Hill, 1964.
- [84] W.-K. Tung, *Group theory in physics*. Philadelphia: World Scientific, 1985.
- [85] V. S. Varadarajan, *Lie groups, Lie algebras, and their representations*. Prentice-Hall series in modern analysis, Englewood Cliffs/N.J.: Prentice-Hall, 1974.
- [86] D. A. Varshalovich, A. N. Moskalev, and V. K. Khersonskii, *Quantum theory of angular momentum: irreducible tensors, spherical harmonics, vectors coupling coefficients, 3nj symbols*. Singapore: World Scientific, 1. repr ed., 1989.

-
- [87] H. Weyl, *The classical groups: their invariants and representations*, vol. 1 of *Princeton mathematical series*. Princeton: Princeton Univ. Press, 2. ed., with suppl ed., 1946.
- [88] H. Weyl, *Gruppentheorie und Quantenmechanik*. Leipzig: Hirzel, 1928.
- [89] E. P. Wigner, *Group theory and its application to the quantum mechanics of atomic spectra*, vol. 5 of *Pure and applied physics*. New York, NY: Academic Press, expanded and improved ed ed., 1959.
- [90] H. T. Williams and C. J. Wynne, “A new algorithm for computation of SU[₃] Clebsch–Gordan coefficients,” *Computers in Physics*, vol. 8, pp. 355–359, May 1994.
- [91] A. Yong, “What is... a young tableau?,” *Notices of the AMS*, vol. 54, pp. 240–241, February 2007.
- [92] D. P. Zelobenko, *Compact Lie groups and their representations*, vol. 40 of *Translations of mathematical monographs*. Providence, RI: American Math. Soc., 1973.
- [93] L. Zuo, M. Humbert, and C. Esling, “An effective algorithm for calculation of the Clebsch–Gordan coefficients,” *Journal of Applied Crystallography*, vol. 26, pp. 302–304, Apr 1993.
- [94] M. A. A. van Leeuwen, A. M. Cohen, and B. Lisser, “Information about LiE.” <http://www-math.univ-poitiers.fr/~maavl/LiE/>, accessed Oct 12 2009.
- [95] PDG, “Clebsch-gordan coefficients, spherical harmonics, and d-functions.” <http://pdg.lbl.gov/2008/reviews/clebrpp.pdf>, 2008.
- [96] U. Fano and G. Racah, *Irreducible Tensorial Sets*. New York: Academic Press, 1959.

Acknowledgements

First of all, I would like to thank my advisor, Jan von Delft. Jan, you did a great job.

Among the people who helped me with my work, I am indebted to Pascu Moca, Andreas Weichselbaum, and Gergely Zaránd.

Thanks to all the people at our chair, who made my life here enjoyable, including Benjamin Abel, Florian Bauer, Barbara Englert, Alexandre Faribault, Peter Fritsch, Vitaly Golovach, Cheng Guo, Theresa Hecht, Georg Heinrich, Markus Heyl, Alexander Hoffmann, Andreas Holzner, Ferdinand Helmer, Jan Heyder, Stefan Kehrein, Stefan Kessler, Sebastian Kronmüller, Björn Kubala, Max Ludwig, Florian Marquardt, Michael Möckel, Clemens Neuenhahn, Korbinian Paul, Jiang Qian, Jérôme Rech, Hamed Saberi, Constantin Tomaras, Maximilian Treiber, Pei Wang, Irek Weymann, and Oleg Yevtushenko.

Then, I would specially like to thank Mrs Kaiser, our secretary. You make the little world of our chair go round.

A special mention deserve Markus Hanl and Wolfgang Münder, my office mates. You made work a lot more enjoyable.

I would like to thank my parents Ursula Alex and Wulf Alex, and my brother Björn Alex, for helping me grow up (and for the dough!).

Finally, a cordial “Thank you!” goes to all my friends, especially Martin Bäuml, Cristian Gohn-Kreuz, Roland Grein, Jona Hampe, Jakoba Heidler, Anne Keck, Daniel Keck, Josef Klingele, Katja Kücherer, Dirk Lange, Julia Parrisius, Christian Schäfer, Katrin Schäfer, Florian Stenzel, Philipp Treiber, Mareike Trunk, and Verena Wild. I always enjoy spending time with you.

Words cannot express how much I would like to thank Sarah.